Title
Single-Cell Analysis of Smooth Muscle Cells

Author
Dai, Tiffany

Publication Date
2016

Peer reviewed|Thesis/dissertation

Single-Cell Analysis of Smooth Muscle Cells

by

Tiffany Dai

A dissertation submitted in partial satisfaction of the

requirements for the degree of

Joint Doctor of Philosophy

with the University of California, San Francisco

in

Bioengineering

in the

Graduate Division

of the

University of California, Berkeley

Committee in charge:

Professor Song Li, Chair

Professor Ming C. Wu

Professor Randall Lee

Fall 2016

Single-Cell Analysis of Smooth Muscle Cells

Abstract

Single-Cell Analysis of Smooth Muscle Cells

by

Tiffany Dai

Joint Doctor of Philosophy

with the University of California, San Francisco

in Bioengineering

University of California, Berkeley

Professor Song Li, Chair

Smooth muscle cells (SMCs) have been heavily implicated in the progression of vascular disease: aberrant proliferation of SMCs leads to narrowing of the blood vessel, and deposition of ectopic calcified deposits compromises the structural integrity of the vessel wall. Since the 1960s, scientists have characterized SMCs as a largely inactive homogeneous population that dedifferentiates to become proliferative and migratory upon vascular injury. However, other studies have suggested that the tunica media layer is comprised of separate subpopulations of SMCs that are not interchangeable. Furthermore, the source of SMCs in atherosclerotic plaques and neointima formation has been proven to be oligoclonal, or derived from a few cells; dedifferentiation of SMCs, which experts describe as a widespread and escalating process undergone by SMCs, should result in a distinctly polyclonal origin of SMCs in neointima and plaques. To investigate heterogeneity among SMCs, single-cell analysis was necessary. For our experiments, RFP+ SMCs were dissociated from the aorta of SMMHC-CreER^{T2}/LoxP-tdTomato transgenic mice and immediately used for strict primary culture or lysis of cell contents. Single-cell analysis of functional contractility showed that although all SMCs were contractile, the level of contractile force was heterogeneous among SMCs. Moreover, the levels of cell traction force and contractile force after exposure to a vasoconstrictor peptide did not correlate with the expression level of essential contractile proteins, α-SMA, CNN-1, or SMMHC. These results indicated that the common practice of characterizing phenotypes of SMCs based on contractile state may be misguided, and direct assessment of the pathogenic behavior of SMCs, such as proliferation and differentiation, may be more appropriate to defining subpopulations of SMCs. To optimize the efficiency of obtaining single-cell clones, we integrated optoelectronic tweezers (OET) with a micropatterned substrate designed for clonal culture. Using the light-induced dielectrophoretic force of OET, single SMCs were selected and positioned in an array of ECM-conjugated islands surrounded by PEG. Through behavioral analysis of single-cell clonal colonies, two

subpopulations of SMCs were distinguished: proliferative and migratory SMCs that were capable of osteogenic differentiation and calcium-phosphate deposition as well as non-proliferative SMCs with extensive cell spreading and no differentiation potential. Additionally, the protein expression of SMCs from the native vessel and from primary culture were compared through immunostaining of cultured clones and single-cell Western blotting of cells that were dissociated from tissue and directly analyzed. From the protein expression profiles of SMMHC and α-SMA, we determined that clustering individual SMCs based on proliferative potential, protein expression of SMCs from normal vasculature, or protein expression of SMCs in primary culture all outlined the same subpopulations of SMCs. Therefore, SMCs are heterogeneous within the normal blood vessel wall. Our body of evidence suggests that only a minority subpopulation of SMCs is capable of undergoing dedifferentiation to proliferate or osteogenic differentiation to deposit ectopic calcium. Consequently, upon perturbation to the vessel wall, these phenotypically plastic SMCs may launch the response of proliferation and differentiation that leads to the progression of vascular disease.

Single-Cell Analysis of Smooth Muscle Cells

Table of Contents

List of Figures

Chapter 1: Introduction

Chapter 2: Establishing an Optoelectronic Tweezers Platform for Patterning of Single Cells on a Microfabricated Surface

Chapter 3: Single-Cell Contractility Assay and Single-Cell Clonal Analysis of Smooth Muscle Cells

List of Tables

Acknowledgments

First and foremost, I would like to thank my advisor, Professor Song Li, for his guidance and encouragement. He taught me to consider the bigger picture, and he instilled in me the confidence to tackle established paradigms. I would also like to thank my other dissertation committee members, Professor Ming C. Wu and Professor Randall Lee, for their constructive feedback and support. One of the highlights in my graduate research was working with knowledgeable and insightful collaborators, Dr. Shao Ning Pei from Professor Ming C. Wu's lab, Elisabet Rosàs from Professor Amy Herr's lab, and Ivan Pushkarsky from Professor Dino Di Carlo's lab. I would also like to thank all Li lab members for the helpful discussions about research as well as the entertaining outings outside of work. In particular, I would like to thank Zoey Huang, Weixi Zhong, and Shao Ning Pei for always brightening my day.

I am incredibly grateful to my parents for providing the best support system. It has been a blessing to study so close to home, enabling us to have frequent visits and funny conversations. I would also like to thank all four of my grandparents, who have the kindest hearts and quickest wits. Above all, I would like to thank my fiancé, JooChuan Ang, for filling our home with love and laughter at the end of every day. Meeting my better half in graduate school and sharing our experiences has been extraordinary. The love from all of you has buoyed me to thrive in any situation.

Chapter 1: Introduction

1.1 Background

Cardiovascular disease is the leading cause of death globally, resulting in 17.3 million deaths per year worldwide and costing $316.6 billion annually in the United States alone[1]. Fatalities often result from the inability of the vascular network to supply the necessary nutrients to downstream organ systems due to vascular disease. The hallmarks of vascular disease are blockage of blood flow or formation of plaques: narrowing of the blood vessel opening causes reduced blood flow, and fatty or calcified deposits in the vessel wall compromise the structural integrity of the blood vessel[2]. The blood vessel wall contains three discrete concentric layers: the tunic intima, which is a monolayer of endothelial cells (ECs); the tunica media, which consists of a thick layer of smooth muscle cells (SMCs); and the tunica adventitia, which is largely comprised of connective tissue and fibroblasts. SMCs are highly non-proliferative and non-migratory under normal conditions. Upon vascular injury, during which the passivating layer of ECs is disrupted, neointimal hyperplasia occurs: SMCs aberrantly proliferate into the lumen through which blood passes[3]. The distinct boundary between the media and intima layers becomes disordered, as SMCs invade the intima layer to form neointima. As a consequence, blood flow is diminished or completely blocked. During the development of atherosclerotic plaques, SMCs promote the maturation of a fatty streak into a plaque in the vessel wall. SMCs become proliferative and migratory, and they participate in the deposition of calcium-phosphate and lipids[4]. SMCs are arguably the most pathogenic cell type in the progression of vascular disease.

In the 1970s, the theory was introduced that SMCs dedifferentiate upon perturbation to the vessel wall: SMCs typically maintain an inactive contractile phenotype, but upon vascular injury, they dedifferentiate into a proliferative and migratory phenotype[5]. In the 1990s and early 2000s, researchers investigated whether SMCs are heterogeneous within the normal uninjured vessel wall[6]. They posited that the majority of SMCs are terminally differentiated contractile SMCs, but an inherently immature subpopulation of SMCs retains the plasticity to launch the proliferative and migratory response that is observed in vascular disease. Studies indicated that the origin of SMCs in neointima and plaques is oligoclonal, or derived from a few cells[7-9]. These results directly contradicted the model of SMC dedifferentiation, for if SMCs were a homogenous population that dedifferentiated as a whole, the source of SMCs in vascular disease would be markedly polyclonal. Moreover, the overuse of bulk techniques further masks the possibility of SMC heterogeneity. In order to discern whether SMCs contain a particularly pathogenic subpopulation, single-cell analysis of SMCs is critical.

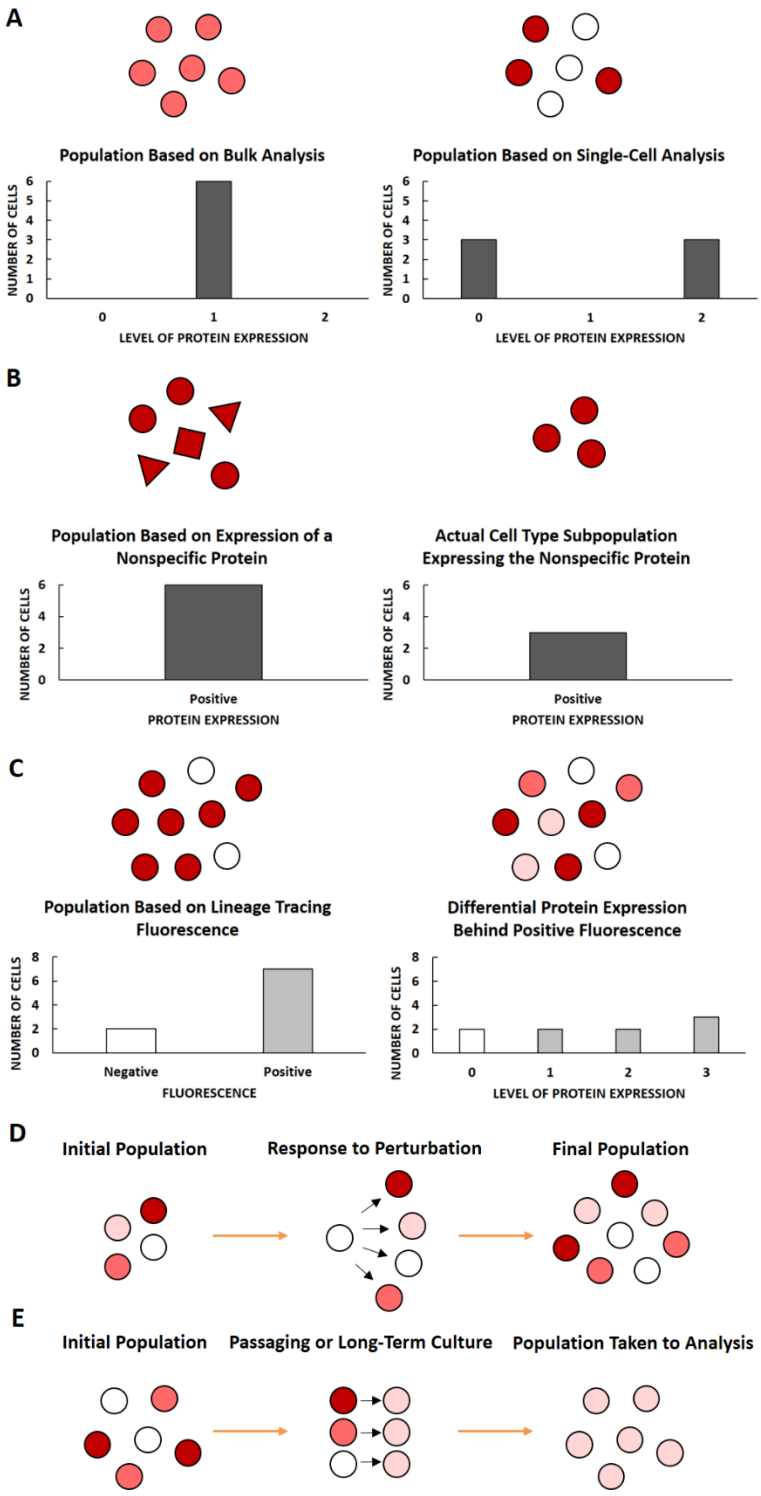

Figure 1.1. Prevalent issues with conventional bulk techniques versus single-cell techniques. Traditional experimental procedures lead to a blended population parameter, derived from the average of its subpopulations. Analysis of live-cell behavior and protein expression on a single-cell level is necessary to determine true cellular response.

Although smooth muscle cells have been investigated for decades, experts in the field currently concede that scientists must advance toward more rigorous experimental design[10]. Bulk techniques, such as Western blots or traditional cell culture in a dish, report blended or averaged parameters. As seen in Figure 1A, analyzing a cell culture in bulk may give the impression that the culture is homogenous, containing cells with an equal level of protein expression, but in actuality, the culture contains two heterogeneous subpopulations whose averaged levels of protein expression is observed using bulk techniques. Only analyzing the culture on a single-cell level would accurately report the two extremes in protein expression level. For example, the media layer of blood vessels has long been regarded as a homogenous layer of SMCs[5]. However, some studies have shown that atherosclerotic plaques originate from a few cells[7,8]. These results suggested that SMCs may in fact be heterogeneous, with a subpopulation that is predisposed toward pathogenesis. Even so, studies on SMCs still treat SMCs as a homogenous population that exhibits a contractile phenotype until injury, upon which all SMCs dedifferentiate into a synthetic phenotype for polyclonal pathogenesis[11].

Another prevalent issue is depicted in Figure 1B: publications often identify a cell type using a well-known protein marker and base their conclusions on observed changes in that sole protein marker. In particular, studies on SMCs often follow convention and use only smooth muscle alpha actin (α-SMA) to distinguish SMCs, but other cell types such as myofibroblasts and macrophages are also known to express α-SMA[12,13]. Figure 1B demonstrates how the expression of a nonspecific protein may inflate the actual number of cells of a particular cell type. Taken a step further, the assessment of a cellular response of the desired cell type may be further skewed. Consequently, it remains difficult to discern which cell types act individually or cooperatively in the development of vascular disease.

Lineage-tracing techniques to label cells expressing relevant markers in transgenic mice have recently been gaining momentum. In cardiovascular studies, this trend is a marked improvement in methodology, as it provides insight into the original source of neointimal and ectopic cells. Nevertheless, the vast majority of published studies on SMCs either does not utilize lineage tracing, or does not perform strict lineage tracing of mature SMCs (e.g. labeling of the exclusive marker SMMHC, smooth muscle myosin heavy chain, rather than the nonspecific marker α-SMA). Furthermore, Figure 1C presents a potential downside to lineage tracing. If a cell expresses the marker of interest, it will be labeled with fluorescence; however, a caveat exists that positively labeled cells may actually have differential levels of protein expression. The left panel of Figure 1C shows the two populations, a minority of negative cells and a majority of positive cells, that would be observed through lineage tracing. The right panel indicates what may actually be occurring: the population of positive cells contains subpopulations with varying protein expression levels, and these subpopulations may be phenotypically heterogeneous as well. Single-cell techniques are necessary to parse out these subpopulations and their individual responses.

Another advantage of single-cell techniques is the ability to discern whether a minority subpopulation is responsible for the majority response of a population to perturbation. Figure 1D illustrates the idea of population demographics remaining the same before and after responding to a cue, which would be reflected as no change in overall protein expression level. Bulk techniques may imply that the population as a whole responds equally, but in reality, one

subpopulation launches a prominent response. For example, vascular stem cells may respond to injury through proliferating as well as differentiating into synthetic and contractile SMCs. Alternatively, a quiescent subpopulation of SMCs may respond to perturbation by proliferating and dedifferentiating, whereas the remainder of SMCs are terminally differentiated. In order to distinguish which cellular subpopulations act as the driving force behind disease development, populations must be tracked at a single-cell level.

Conventional cell culture methods involve weeks of expansion and numerous passages before analysis: labs often purchase cell lines, or if they harvest fresh tissue, cells migrate from tissue explants over the course of weeks and are passaged multiple times before use in assays. Figure 1E depicts the changes that may occur through passaging and time in culture. For example, if the initial population is a heterogeneous population of vascular stem cells and contractile SMCs, the population may shift to a homogenous population of synthetic SMCs as stem cells differentiate and contractile SMCs dedifferentiate. Scientists sometimes describe in their methodology that they limit cells to five passages, but that already provides ample time for the population makeup to change dramatically. If experiments are conducted on cells that are no longer reflective of the original population, conclusions cannot be drawn about the mechanism behind disease and cellular response to potential therapies.

1.2 Outline

This biological investigation identifies subpopulations of SMCs and examines their ability to contribute to the progression of vascular disease. By overcoming the limitations of existing cell culture methods and studying this biological problem from a unique single-cell perspective, we provide compelling evidence of a particularly pathogenic subpopulation of SMCs that resides within the native vessel wall.

In Chapter 2, a novel platform for clonal culture of single cells was developed: optoelectronic tweezers (OET) was integrated with a micropatterned substrate of extracellular matrix (ECM) and polyethylene glycol (PEG). Through light-induced dielectrophoretic force, OET was used to manipulate single cells into an array of ECM islands surrounded by cell-inhibitory PEG. Single-cell positioning via OET greatly enhanced the efficiency of obtaining single cells per ECM island compared to the passive technique of random seeding. OET provided an active manipulation technique in which a projected light pattern was readily reconfigurable in real-time in response to the desired arrangement and directional movement of cells.

In Chapter 3, SMCs were derived from the aorta of SMMHC-CreER^{T2}/LoxP-tdTomato transgenic mice and thus labeled with red fluorescence. The cells were freshly dissociated from native ECM immediately prior to experiments for strict primary culture. First, the functional contractility of SMCs was analyzed on a single-cell level. We observed that all SMCs were contractile, but the level of contractile force from various individual SMCs was heterogeneous. Furthermore, the level of cell traction force on the substrate or contraction force upon exposure to endothelin-1 (ET-1), a vasoconstrictor peptide, did not correlate with the expression level of contractile proteins, such as α-SMA, CNN1, and SMMHC. Studies on SMCs assume that the expression of contractile proteins represents the differentiated contractile phenotype of SMCs. Though these proteins are critical components of the contractile apparatus of SMCs,

the expression level of these contractile proteins did not dictate the level of functional contractility observed in the respective single SMCs. Additionally, single-cell behavioral analysis of SMCs showed that the majority of SMCs were terminally differentiated and non-proliferative, and a minority subpopulation of SMCs was proliferative and migratory. Non-proliferative SMCs also exhibited significantly larger cell surface area than proliferative SMCs. Proliferative SMCs were capable of differentiating into osteoblasts and generating calcium deposits, whereas non-proliferative SMCs could not undergo osteogenic differentiation. Neither proliferative nor non-proliferative SMCs were able to undergo adipogenic differentiation. Therefore, behavioral analysis of single SMCs and their clonal colonies showed that a subpopulation of SMCs may launch the robust response of proliferation, migration, and widespread mineralization observed in the progression of vascular disease.

In Chapter 4, the expression level of contractile protein markers was analyzed on a single-cell level in primary culture and in the native vessel. Using single-cell Western blotting, the protein expression profile of SMMHC, CNN1, and α-SMA was probed and plotted for each SMC. The SMCs were lysed and analyzed immediately after dissociation from tissue; thus, the quantified protein levels reflected the expression of SMCs in the normal blood vessel wall without exposure to culture. Using the k-means method, we determined that the relationship between SMMHC and α-SMA was most influential to the clustering of SMCs based on protein expression. To compare the protein expression of SMCs from the native vessel to SMCs in primary culture, SMCs from clonal culture were also co-stained for SMMHC and α-SMA. Because we were able to observe the behavior of SMCs in culture before staining, we also had information on the proliferative potential of each SMC. First, we applied k-means clustering to all of the SMCs in the immunostaining intensity plot of α-SMA versus SMMHC, and two clusters were outlined. Next, we overlaid the two clusters with the proliferative and non-proliferative groups to see how well the differential behavior correlated with differential protein expression. The plots correlated extremely well. Lastly, we further overlaid the single-cell Western blotting plot of α-SMA versus SMMHC after applying k-means clustering to those data points as well. The clusters matched exactly, thus indicating that the distribution of protein expression among SMCs in primary culture was retained from the native vessel. Consequently, SMCs are naturally heterogeneous within the vessel wall. The subpopulations of SMCs exhibit different proliferation rates, differentiation potential, and levels of contractile protein expression. The aberrant proliferation and ectopic differentiation of a minority subpopulation of SMCs promote the development of vascular disease.

Chapter 2: Establishing an Optoelectronic Tweezers Platform for Patterning of Single Cells on a Microfabricated Surface

2.1 Introduction

2.1.1 Optoelectronic Tweezers

Optoelectronic tweezers (OET) offers high-resolution manipulation of particles through light-induced dielectrophoresis[14]. Dielectrophoresis (DEP) describes the force experienced by a polarizable particle when exposed to a non-uniform electric field. The amount of force varies depending on the shape and size of the particle, the frequency of the electric field, and the electrical properties of the particle and surrounding medium. Generally, a homogenous spherical particle immersed in a conductive medium will experience a time-averaged dielectrophoretic force[15]:

$$F_{dep} = 2\pi r^3 \varepsilon_m \,\mathrm{Re}\left\{\frac{\varepsilon_p^* - \varepsilon_m^*}{\varepsilon_p^* + 2\varepsilon_m^*}\right\} \nabla \left|\vec{E}_{rms}\right|^2$$

The variable r is the radius of the particle, $\vec{E}_{rms}$ is the root-mean-square electric field strength, ε_p^* is the complex permittivity of the particle, and ε_m^* is the complex permittivity of the medium. The Clausius-Mossotti function in brackets illustrates how the DEP force is frequency-dependent. Complex permittivity ε^* is dictated by ω as angular frequency, σ as electrical conductivity, and ε as permittivity:

$$\varepsilon^* = \varepsilon - \frac{i\sigma}{\omega}$$

Therefore, the chosen frequency of the applied electric field influences the complex permittivity of the particle and medium, and depending on whether the complex permittivity of the particle is higher than that of the medium or vice versa, the real part of the Clausius-Mossotti factor will be positive or negative, respectively. Consequently, the particle will experience either positive DEP as it is attracted to the electric field maxima or negative DEP as it is repelled by the electric field maxima. Additionally, the Clausius-Mossotti function expresses how the magnitude of the DEP force can be maximized by increasing the difference between the complex permittivity of the particle and that of the surrounding medium.

Because cells are less homogenous than particles, the complex permittivity of the particle ε_p^* is adjusted to reflect the cell as its cytoplasm within its cell membrane, or an inner sphere nested in an outer shell[16]:

$$\varepsilon_p^* = C_{shell}^* \frac{r\varepsilon_{core}^*}{\varepsilon_{core}^* + rC_{shell}^*}$$

The variable r is the radius of the cell, ε_{core}^* is the complex permittivity of the cytoplasm, and C_{shell}^* is the complex capacitance of the cell membrane:

$$C^*_{shell} = \frac{\varepsilon_{shell}}{d} - j\frac{\sigma_{shell}}{d}$$

With the adjustment in ε^*_p and thus the Clausius-Mossotti factor, the overall dielectrophoretic force experienced by the cell is affected as well.

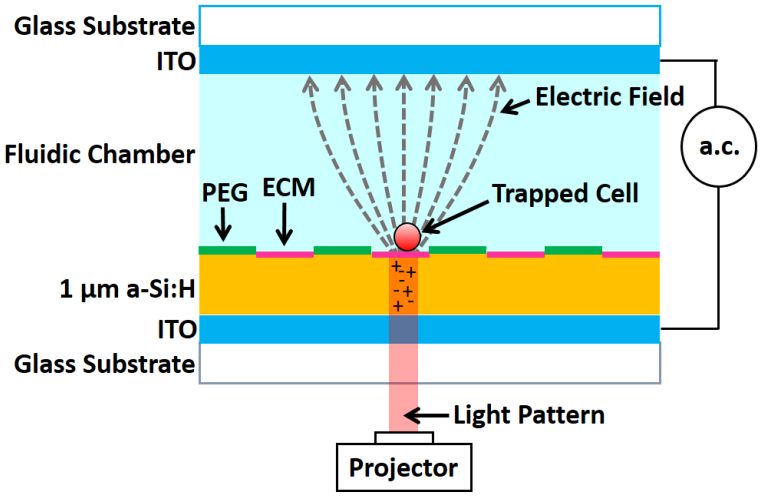

Figure 2.1. Cell manipulation using optoelectronic tweezers (OET). An AC electric field is applied, and a light pattern is projected onto an area of the substrate. A local dielectrophoretic (DEP) force is exerted on a nearby cell that can be subsequently trapped and positioned.

Optoelectronic tweezers is set up as shown in Figure 2.1. The substrate consists of glass, indium tin oxide (ITO), and amorphous silicon (a-Si:H). The photoconductive surface is a critical element of OET operation. When an optical pattern from a light source, such as a data projector, is shone onto the photoconductive a-Si:H-coated chip surface, the electric field in the area of the light pattern is locally modified. Photons of visible light from the projected light pattern generate electron-hole pairs in the silicon layer. The resulting cloud of electrons and electron holes remains localized to the lit area of the amorphous silicon. With the applied electric field, the cloud orients itself so that the electrons$^-$ and holes$^+$ are polarized, and the electron cloud functions as carriers. As a result, the lit area of the a-Si:H layer becomes conductive, and the ITO layer underneath is essentially exposed. Consequently, a dielectrophoretic force is exerted on nearby cells, which can then be corralled and controlled by the light pattern.

2.1.2 Single-Cell Analytical Techniques

	Cell Selection	Long-term Culture	Cell Containment	Pure Populations
Serial Dilution	✗	✓	✗	✗
Physical Traps	✗	✗	✓	✗
FACS	✓	✓	✗	✗
OET	✓	✓	✓	✓

Table 2.1. Advantages and pitfalls of existing single-cell techniques. Commonly used methods for single-cell analysis, such as serial dilution and physical traps, rely on random seeding or random flow, which results in nonspecific cell selection. Current devices predominantly separate single cells for immediate lysis and analysis without long-term live-cell analysis through cell culture. OET can be adapted to fill the need for an active manipulation technique providing single-cell selection, positioning, and quantitative analysis in lieu of these passive techniques.

Developing a tool for systematic analysis of single cells and the behavior of clonal colonies is necessary in order to distinguish the roles of different cell types or different subpopulations within a cell type. Conventional cell culture methods may mask the significance of a particularly pathogenic minority population due to the averaging effects of bulk techniques.

Existing single-cell techniques present certain advantages and disadvantages (Table 2.1). The most commonly used method of separating single cells is serial dilution, in which clonal populations are generated by diluting cells to an extremely low cell density in order to track a cell and its daughter cells in each well of a 96-well plate[17]. In practice, this technique is extremely unreliable and inefficient: the vast majority of wells often contains no cells, and it is difficult to guarantee that only one cell is in a well[18]. Furthermore, one cell in culture may exhibit low cell viability, as some cell types require at least a low cell density in culture to survive[19,20]. An improved method would maintain separation among the clonal colonies while allowing the cells to grow in the same culture. Additional restrictions of serial dilution include the inability to constrain and track cells: as cells proliferate and migrate, the colony risks unknown contamination by other colonies in the well. Moreover, tracking live-cell behavior, such as proliferation rate over time in culture, would be simpler with indexed and contained colonies. Similarly, the random nature of cell seeding does not allow for the selection of specific cells, such as a fluorescently labeled cell type, to culture at specific addresses. Precise cell selection is a central requirement when the cell type of interest is a minority in a heterogeneous whole population.

Another common technique with single-cell resolution is fluorescence-activated cell sorting (FACS). Cells in suspension are separated into single cells and sorted based on size and fluorescence[21]. FACS is particularly useful when a target population is labeled in fluorescence through immunostaining or transgenes, as the cell type of interest can then be purified from a heterogeneous cell culture. However, the specificity of cell selection by FACS

is limited to the specificity of fluorescent labeling. For example, cell markers are often expressed by different cell types, and it may be difficult to find an antibody that exclusively labels the cell type of interest. Similarly, if subpopulations exist within a cell type, they will all express the same general markers of that cell type. In that scenario, if FACS is used for only end-point analysis, the subpopulations will all be labeled positive, and heterogeneity within a cell type will be masked; quantification of FACS results is commonly reported as percentages of positive or negative cells. On the other hand, when FACS is used for subsequent cell culture, scientists often treat sorted cells as a homogenous culture under the assumption that sorted cells are purified. However, a purified cell type from FACS should not be assumed homogenous: single-cell sorting does not preclude conventional cell culture from masking the individual contributions of subpopulations. Moreover, FACS allows for a higher percentage of purity but does not completely exclude contamination by other cells, and the influence of contaminating cells may be a confounding factor that is difficult to discern in bulk culture. Consistent single-cell analysis throughout an experiment is necessary for true characterization of a population.

Previous strategies to overcome these obstacles include flowing or settling single cells into physical traps. For example, cells in suspension are settled into microwells with a diameter to fit single cells and exclude cell clusters[22]. Another such device catches and confines cells in an array of U-shaped PDMS barriers[23]. Nevertheless, these systems still operate on random flow and thus produce an array with nonspecific cell selection. The passive nature of these devices does not allow for active positioning or targeting, which would optimize the number of single cells and the proportion containing the cell type of interest, respectively. Additionally, these platforms simply were not designed for long-term cell culture, but rather for immediate lysis and analysis of isolated single cells. While analysis of cell content such as gene or protein expression is important, it is also imperative to explain how genotypic differences between subpopulations manifests as distinct phenotypes that may have different roles in disease development. Thus, long-term culture of clonal colonies is necessary for behavioral analysis.

A novel platform integrating optoelectronic tweezers and a microfabricated substrate for single-cell clonal culture can satisfy all of these requirements:

1) Parallel analysis of isolated and indexed single cells in an array
2) Selection of specific cells in suspension, such as a fluorescently labeled cell type
3) Positioning of only one cell in each island of the array using an active manipulation technique, improving upon random surface loading efficiency
4) Compartmentalization of a single cell and its daughter cells within a large extracellular matrix protein (ECM) island for clonal culture (500 μm or 1 mm diameter)
5) Compatibility with common cell culture materials for ease of culture and further biological analysis

OET is a versatile tool for selecting and positioning cells: the projected shape can be readily reconfigured in real-time in response to the desired arrangement and directional movement of the cells[14]. The smallest resolution of the projected light pattern is 13 by 15 μm in area on the substrate. Previously, OET has been used to pattern particles and nanowires[24,25]. For biological applications, Wu lab has also successfully applied OET to the parallel manipulation and simultaneous electroporation of a single-cell array of suspension cells[26]. In

addition, selection of murine embryos for optimal in vitro fertilization (IVF) implant efficiency has been performed[27]. OET has also been tested on motile and non-motile human sperm in order to assess sperm viability[28].

Another advantage of OET is that it functions as an instant, label-free live/dead assay: the porous cell membrane of a dead cell does not respond to the local electric field generated by the light pattern, but live cells respond strongly to the DEP force[14]. This feature of the platform is particularly important when using primary cells that are freshly digested from tissue, since enzymatic digestion typically leads to some cell death. By assessing cell viability before culture, we can select for and position cells that are healthy, further increasing the efficiency of the platform. Other techniques, which primarily form cell arrays through physical trapping, cannot associate a specific cell with a particular position or exclude unhealthy cells before analysis.

The flexibility and programmability of OET, in combination with micropatterned ECM-conjugated islands for clonal culture on the device surface, provide the potential for high-throughput, parallel loading of single cell arrays for extensive culture, characterization, and quantification.

2.2 Materials and Methods

2.2.1 Fabrication of Device Surface for OET Operation and Single-Cell Clonal Culture

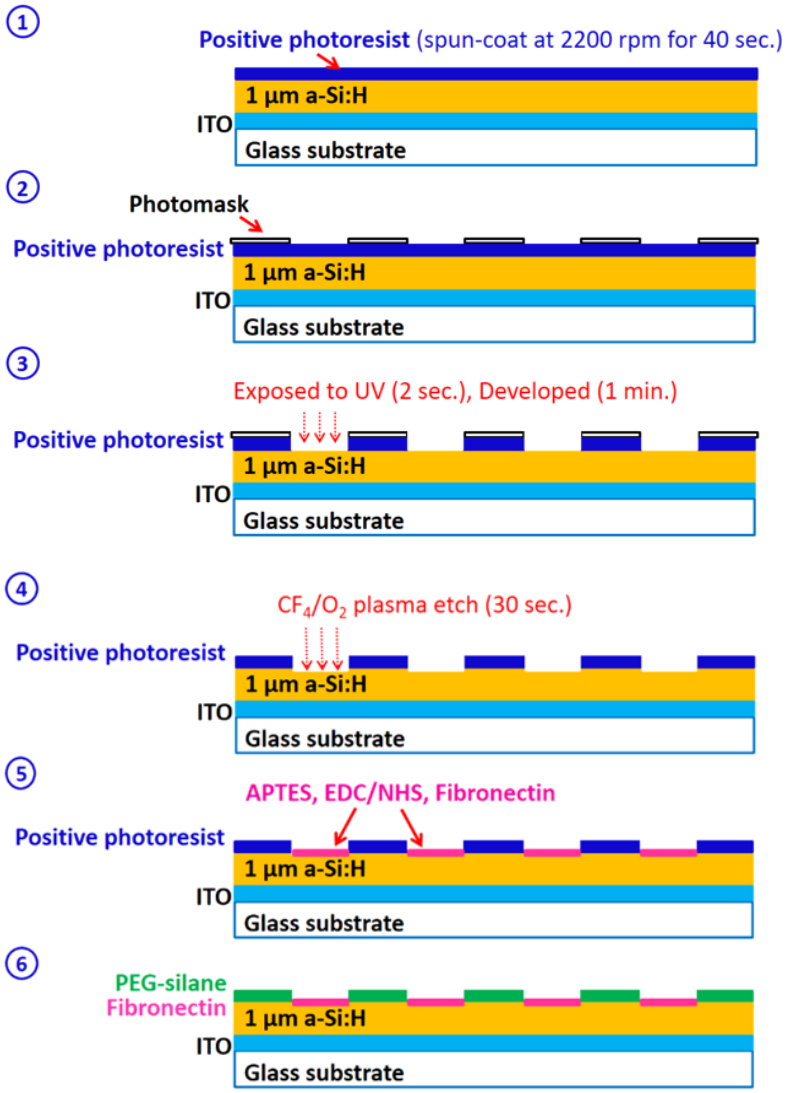

Figure 2.2. Fabrication of device surface compatible with OET functionality and single-cell clonal culture. The elements necessary to OET function (a photoconductive surface and an antifouling surface coating for cell movement) were integrated with the characteristics of a cell culture substrate (an extracellular matrix protein coating for cell attachment). PEG and fibronectin were covalently conjugated and patterned onto the device surface to provide a substrate for single-cell clonal culture.

A micropatterned substrate with an array of extracellular matrix protein (ECM) islands surrounded by an otherwise PEGylated surface was fabricated for the long-term culture of single-cell clonal colonies (Figure 2.2). Basic OET operation required 0.7 mm-thick glass coated with 300 nm-thick indium tin oxide (ITO, a transparent conductive material), which was then deposited with 1 µm of amorphous silicon (a-Si:H) via plasma-enhanced chemical

vapor deposition (PECVD). The substrate was treated with oxygen plasma for 10 min. to clean the surface of organic contaminants. Next, g-line positive photoresist was spun onto the surface at 2200 rpm for 40 s to form a 2 µm layer of photoresist. After a soft-bake at 90ºC for 1 min., a photomask with an array of 500 µm-diameter or 1 mm-diameter vias was placed in direct contact with the surface of the substrate. The substrate was exposed to UV for 2 s and then immersed in g-line photoresist developer under gentle agitation for 1 min. Using CF_4/O_2 plasma of reactive ion etching (RIE), the surface was slightly etched 100 nm in height within the arrayed islands in order to visualize the location of the islands under brightfield during cell positioning and subsequent analysis. The substrate was exposed to 30 s of CF_4/O_2 plasma at 50% power for etching and then 1 min. of O_2 plasma at 20% power for cleaning and hydroxylation. The exposed areas of the surface were aminosilanized with APTES (3-aminopropyltriethoxysilane; Sigma, 440140) under vacuum for 1 h and annealed at 100ºC for 10 min. Subsequently, the substrate was incubated with 0.2 M EDC (1-ethyl-3-(-3-dimethylaminopropyl) carbodiimide hydrochloride; Sigma, E1769), 0.5 M NHS (N-hydroxysuccinimide; Sigma, 130672), and 50 µg/mL fibronectin (Sigma, F1141) in 1X PBS (phosphate buffered saline) for 1 h at 37ºC in order to covalently conjugate fibronectin to the surface within the islands of the array. Lastly, the photoresist was stripped, and the substrate was thoroughly rinsed in water. The substrate was coated with 1.5% silane-functionalized polyethylene glycol (PEG-silane; Laysan Bio, MPEG-SIL-30K) in 95% ethanol overnight at 65ºC and rinsed thoroughly. The modified substrate surface was then ready for use, and to complete the device, an ITO-coated glass top cover was placed on top of the substrate above a 100 µm spacer.

If completely transparent vias were preferred, such as for future dye-based staining of cellular byproducts, exposure to CF_4/O_2 plasma of RIE was increased to 3 min. in order to etch away the entire silicon layer within the vias. The substrate was still subjected to a subsequent 1 min. of O_2 plasma for cleaning. Because gas flow within the RIE chamber is uneven, the vias were then held to the light to check for incomplete etching. If any vias were only partially etched, the substrate was exposed to another 1 min. of CF_4/O_2 plasma and 1 min. of O_2 plasma. Next, the ITO was etched from within the vias using hydrochloric acid (HCl). Equal parts of aqueous HCl and water were combined to make a 18.5% HCl solution. The substrate was immersed in the solution under gentle agitation for 15 min., rinsed extensively in water, and dried. Conductivity was assessed to confirm that the ITO layer had been etched. Subsequent steps for ECM and PEG conjugation remained the same.

Top covers were cut from an ITO-coated glass sheet. A hole was drilled into the center of each top cover. The ITO-coated side was covered in 1.5% PEG-silane in 95% ethanol overnight at 65ºC and rinsed thoroughly. Silver epoxy was coated on both sides and at the edges of one corner of each top cover and cured at 65ºC; this corner allowed for topside electrical contact with the ITO-coated side of the top cover, which was placed face-down when assembled above the substrate. A syringe needle tip was filled with polydimethylsiloxane (PDMS) and aligned with the drilled hole in the top cover, with the path between the drilled hole and syringe tip kept open with a needle as the PDMS cured at room temperature overnight. The modified top cover allowed for gradual exchange of media using a syringe pump without disturbing the positioned cells.

2.2.2 OET Operation

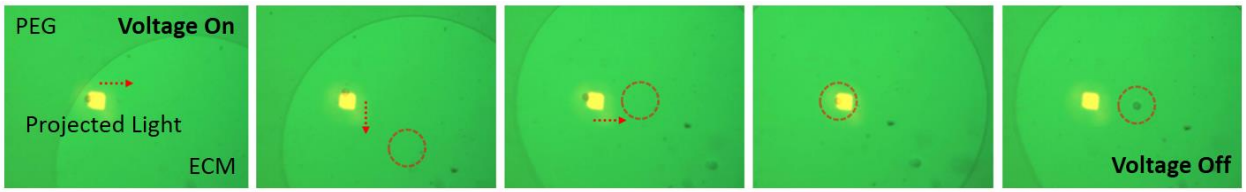

Figure 2.3. Selection and positioning of a single cell in an ECM island via OET. Arrow indicates directional movement of the light pattern. Circle indicates same spot in the island as field of view changes. At 10 V_{ppk} and 100 kHz, the cell was attracted to the projected light and was positioned in the center of the ECM island by shifting the light pattern.

The device was assembled with a top cover and 100 µm spacer above the micropatterned substrate with an array of ECM islands surrounded by PEG. Cells suspended in low-conductivity media, which was previously equilibrated to 5% CO_2 and 37ºC in a cell culture incubator, were flooded into the fluidic chamber. Low-conductivity media (BTX, 47-0002) was used because the liquid conductivity of the fluidic layer must be lower than 100 mS/m for OET operation. An AC electric field was applied, and at 10 V_{ppk} and 100 kHz, cells experienced a positive DEP force (Figure 2.3). Single cells were selected and positioned within ECM islands on the device surface. Throughout the process, cells in the device were maintained at 37ºC on a heated stage. After cell positioning, the device was submerged in cell culture media that was previously equilibrated to 5% CO_2 and 37ºC by filling the surrounding petri dish. Next, cell culture media was gradually perfused into the fluidic chamber of the device through the syringe tip attached to the top cover. Cell culture media consisted of Dulbecco's Modified Eagle Medium (DMEM) with 10% fetal bovine serum (FBS) and 1% Penicillin-Streptomycin (Pen-Strep). Using a syringe pump, the low-conductivity media was replaced with cell culture media over the course of 1 h without disturbing cell positioning. The timing was experimentally confirmed through previous tests using blue dye. The petri dish containing the device was placed into a cell culture incubator overnight for cell attachment, and the next day, the top cover was gently removed. Subsequently, the substrate was treated as a conventional cell culture: the substrate was cultured in a petri dish in a cell culture incubator, and cell culture media was replaced every other day.

Notably, Wu lab has previously proven that the applied voltage does not affect cell viability: murine embryos subjected to 20 V_{ppk} and 100 kHz during OET manipulation were implanted and resulted in healthy pups[27]. For cell positioning, 10 V_{ppk} and 100 kHz were applied, and empirically, we observed no difference in viability and proliferation rate between cells manipulated with OET and seeded control cultures. Optoelectronic tweezers uses reduced optical power compared to optical tweezers; thus, OET is significantly less harsh on cells while still supplying the same degree of force as optical tweezers, on the scale of tens to hundreds of piconewtons[15]. The optical intensity of OET is low, at 1 watt per cm^2, as measured with a thermopile. Moreover, the silicon layer acts as a screening layer for the projected light; cells are only exposed to the red part of the light spectrum, which is considerably less damaging than UV. Furthermore, possible Joule heating from OET was tested using thermosensitive microgels that swell and shrink reversibly in response to surrounding temperature to an

accuracy of 0.054ºC[29]. 20 V_{ppk} and 1 MHz were applied, and no significant Joule heating was observed.

2.3 Results and Discussion

2.3.1 Selective Patterning of ECM and PEG

Several issues were encountered and resolved while fabricating the micropatterned device surface: 1) For particles and suspension cells, bare silicon was sufficient as a substrate for cell manipulation via OET, but for adherent cells, a high molecular weight (30,000 MW) PEG coating was necessary for fast and consistent movement of the cell in response to dielectrophoretic force. 2) To show the location of ECM-conjugated islands into which single cells were positioned while operating OET, the silicon layer was slightly etched 100 nm in height using CF_4/O_2 plasma; visualization of the array under brightfield imaging was also necessary for subsequent live-cell monitoring and further analysis. 3) Typically, ECM is deposited onto tissue culture plates or glass coverslips through incubation and passive adsorption of protein. However, after assessing fibronectin deposition via immunostaining, it was determined that passive adsorption resulted in an uneven or partially missing coating of ECM within the islands. For single-cell clonal analysis, conditions for cell attachment must be optimal, so stable and consistent coating of ECM was required. The problem was resolved by covalently conjugating fibronectin through aminosilanizing the surface and using EDC/NHS activation.

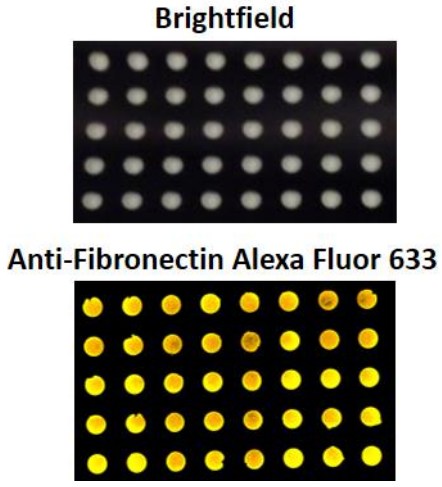

Figure 2.4. Patterned ECM within arrayed islands for OET positioning and long-term cell culture verified through immunostaining. A micropatterned substrate was fabricated with an array of indexable and isolated ECM-conjugated islands on an otherwise PEGylated device surface. Selective ECM deposition within the arrayed islands was confirmed with anti-fibronectin and Alexa Fluor 633 immunostaining.

The top panel of Figure 2.4 shows the modified device surface under brightfield imaging. During fabrication, the silicon layer within the islands was etched before ECM deposition in order to allow for basic brightfield visualization of the array during OET

positioning and subsequent analysis of single-cell clones. Depending on the length of culture and proliferation rate of the desired cell type, the diameter of the islands can be easily altered by switching the photomask; for example, 500 µm islands may be sufficient for live-cell monitoring over the course of a week, but 1 mm islands may be preferable for differentiation assays that extend beyond two weeks.

The lower panel of Figure 2.4 verifies the selective and consistent coating of ECM within the islands. Because cell attachment was critical to the efficiency of establishing single-cell clones, ECM was covalently conjugated rather than passively adsorbed to the substrate. The device surface was hydroxylated through oxygen plasma and then aminosilanized with APTES under vacuum. Incubation in a solution of EDC, NHS, and fibronectin allowed EDC to crosslink the amine-coated surface with the carboxylic acids of the ECM protein; NHS was present to stabilize the intermediate form[30,31]. EDC and NHS covalently conjugated the device surface with fibronectin without incorporating themselves into the final product.

The remainder of the device surface was covalently conjugated with PEG-silane. Because it is a known biologically compatible inhibitor of cell adhesion, PEG was applied outside of the ECM islands; therefore, clonal colonies were contained as cells proliferated. In addition, cells that remained outside of the islands after positioning single cells within the islands did not adhere[32,33]. Coating the device surface with PEG also facilitated the movement of cells in response to OET[34].

2.3.2 Single-Cell Positioning Efficiency of OET versus Random Seeding

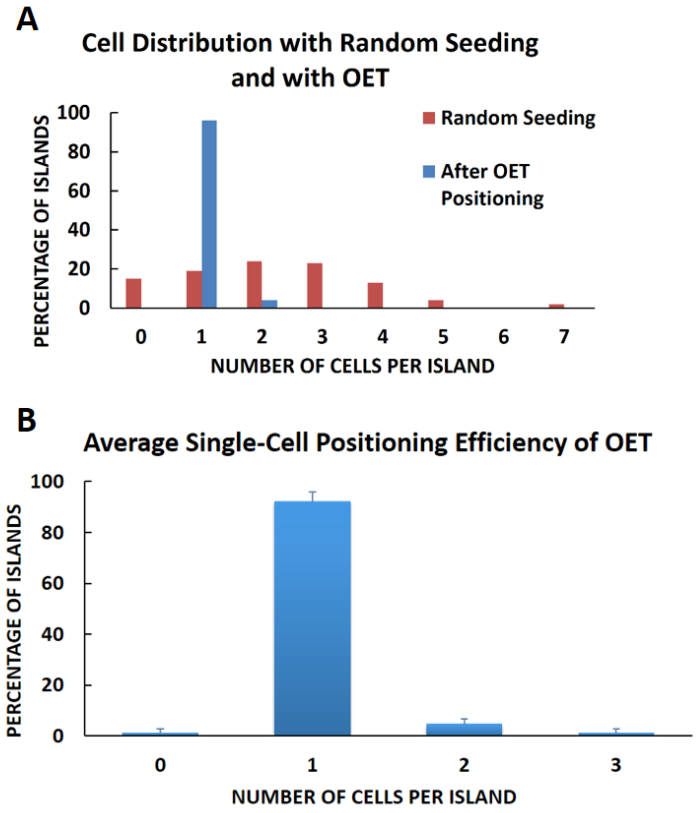

Figure 2.5. Efficiency of obtaining a single cell per ECM island using OET positioning versus random seeding. The percentage of ECM islands containing a single cell increased dramatically after OET positioning compared to initial random seeding.

Figure 2.5a depicts the increased efficiency of obtaining a single cell per ECM island after OET positioning compared to initial random seeding. When cells in suspension were flooded into the fluidic chamber of the device, random seeding resulted in most islands containing multiple cells, primarily with two or three cells each. After OET positioning, 96 islands in the 10 by 10 array, or 96% of islands, contained single cells. For islands that contained multiple cells from random seeding, OET was used to move all but one cell out of the island; for those that contained no cells, OET positioned a single cell within the island.

Random seeding follows a Poisson distribution, which describes the probability of a number of events, such as a single cell, occurring in a fixed interval, such as the area of an ECM island[35,36]. The formula for a Poisson distribution is as follows:

$$P(x) = \frac{(e^{-\lambda})(\lambda^{x})}{x!}$$

The probability $P(x)$ of finding x number of cells at different λ values is described by the formula. λ represents the desired mean number of cells per island, which is $\lambda=1$ for single-cell analysis. x indicates the actual number of cells that will likely be observed per island.

Cell density in suspension can be optimized to obtain a higher number of single cells per island from random seeding; lower cell density would result in a peak at the number of islands containing zero cells, and higher cell density would result in most islands containing two or three cells. According to the Poisson distribution, random seeding at an optimal cell density for single cells would result in approximately 35% of the array containing single cells per island. By comparison, Figure 2.5b demonstrates that the average single-cell positioning of OET resulted in 92% of islands containing single cells.

2.4 Conclusion

Optoelectronic tweezers provided an active manipulation technique that significantly increased the efficiency of obtaining single cells per ECM island over the passive nature of random seeding, which has often been used in other single-cell techniques. The single-cell resolution of OET for cell manipulation allowed for rapid, parallel arraying of cells, as the shape and movement of the light pattern was easily reconfigurable in real-time. By integrating elements of OET with a substrate that was conducive to cell culture, the platform readily facilitated increased efficiency and control in potential biological studies.

Chapter 3: Single-Cell Contractility Assay and Single-Cell Clonal Analysis of Smooth Muscle Cells

3.1 Introduction

3.1.1 The Blood Vessel Wall and Vascular Disease

A critical component of the circulatory system is the network of blood vessels that provides blood flow to various organ systems in the body. The blood vessel wall is comprised of three concentric layers: the tunica intima, tunica media, and tunica adventitia[37]. The tunica intima contains a monolayer of endothelial cells (ECs) that lines the lumen, the opening through which blood passes. The tunica media consists of a thick layer of smooth muscle cells (SMCs), which contract to control blood flow. The tunica adventitia is comprised of fibroblasts and connective tissue. During development, ECs form tubes and recruit SMCs to support and surround the ECs; proper assembly of ECs and SMCs is critical to the formation of functioning blood vessels[38]. Typically, ECs and SMCs have very low proliferation rates[39]: the main function of ECs is to passivate the lumen, rendering the blood vessel unreactive and inert, and SMCs primarily control blood pressure and blood flow. If the discrete layers of the vessel wall become compromised, the ability of the blood vessel network to supply nutrients downstream is severely impacted.

With age, blood vessels become narrower and stiffer. The vessel wall thickens as well as accumulates calcium and fat. The progression of vascular diseases such as atherosclerosis is characterized by two hallmarks, neointimal hyperplasia and atheroma formation[2]. Atheroma formation is the accumulation of lipid droplets and calcium deposits within the vessel wall; these tissue types are ectopic, or abnormal to the resident tissue. Consequently, the presence of unusual debris in the vessel wall leads to a loss of structural integrity and compromises the function of the blood vessel. Neointima hyperplasia by definition is ‘neo’ for new, ‘intima’ for innermost, ‘hyper’ for excessive, and ‘plasia’ for growth. Neointima hyperplasia describes a narrowing or blockage of the lumen by an aggregation of proliferative and migratory smooth muscle cells, restricting blood flow to target organs[40]. In the initial step of vascular disease, low-density lipoprotein is trapped in the vessel wall and internalized by macrophages that become foam cells; the lipid-laden foam cells break down to form fatty streaks. Accordingly, the endothelial cell layer that normally protects the lumen is disrupted. Upon dysfunction of the passivating EC layer, SMCs react to the disturbed cellular microenvironment by migrating into the intima. SMCs form neointima through proliferation and increased deposition of extracellular matrix, thus promoting the maturation of the fatty streak into an organized atherosclerotic plaque[41]. Eventually, the lesion becomes enlarged and covered by a fibrous cap of SMCs. Paradoxically, SMCs in the fibrous cap are essential to the stability of the plaque; if the plaque ruptures, its core of lipids and necrotic tissue enters the bloodstream and potentially causes thrombosis, heart attack, or stroke[42]. Loss of SMCs in the fibrous cap is often due to apoptosis. SMCs have been largely implicated in the vascular remodeling that creates diseased vessels through aberrant proliferation, differentiation, and apoptosis.

3.1.2 Smooth Muscle Cell Dedifferentiation versus Heterogeneity

Under normal conditions, the primary purpose of SMCs is to control blood flow by dilating or constricting the blood vessel. In 1967, Wissler described the tunica media layer of the vessel wall as exclusively comprised of SMCs that have multiple roles: to maintain vascular tone, SMCs are contractile, but SMCs are also responsible for neointima formation through proliferation and migration[43]. During the 1970s, Campbell and Campbell introduced the theory that mature SMCs, which are highly non-migratory and have an extremely low proliferation rate, dedifferentiate into a proliferative and migratory phenotype upon injury[5]. Using electron microscopy, they characterized dedifferentiation as a loss of spontaneous contraction and myofilaments. However, these studies were primarily conducted on visceral SMCs, derived from such as vas deferens, rather than vascular SMCs from blood vessels. Vascular SMCs do not exhibit the same spontaneous contraction. Recent studies have characterized SMCs through the presence of contractile proteins under the assumption that if components of the contractile apparatus are present, SMCs display a contractile phenotype. Alpha smooth muscle actin (α-SMA) is a general marker for SMCs that is expressed throughout the development of SMCs[44]. However, other cell types are known to express α-SMA as well[12,13]. Calponin-1 (CNN1) is expressed later in development of SMCs, but it is also a nonspecific marker[45-47]. Smooth muscle myosin heavy chain (SMMHC) is the most exclusive marker of SMCs that is not expressed by any other cell type during development or in adult tissue[48]. Through lineage tracing of SMMHC, which specifically labels SMCs, multiple groups have shown that after vascular injury, marker expression of contractile proteins was downregulated in SMCs. For example, Nemenoff showed that after wire injury to the femoral artery of SMMHC-CreER^{T2}/R26R-βGal transgenic mice, some SMCs that were negative for α-SMA were observed[49]. Similarly, Regan indicated that after wire injury to the carotid artery of SMMHC-LacZ mice, all SMCs downregulated and no longer expressed SMMHC[11]. In the atherosclerotic plaques of ApoE$^{-/-}$/SMMHC-CreER^{T2}/R26R-eYFP mice, Shankman found SMCs that were negative for α-SMA[50]. Thus, SMCs have been shown to modulate the expression of contractile proteins and participate in vascular remodeling.

The current paradigm states that the tunica media contains a homogenous layer of contractile SMCs in the normal blood vessel, and upon perturbation, SMCs as a whole dedifferentiate and invade the intima layer. In the case of dedifferentiation, as SMCs dedifferentiate from contractile into the proliferative phenotype, the origin of SMCs in neointima or plaques should be polyclonal, or derived from numerous SMCs. However, some studies have suggested that the pathogenic phenotype of SMCs may be ascribed to a pre-existing subpopulation of SMCs in a naturally heterogeneous media layer. A seminal study by Benditt and Benditt showed that SMCs accumulating in human atheromatous plaques were monoclonal or oligoclonal in origin, indicating that only one or a few SMCs proliferated to form the aggregation of SMCs[7]. Additionally, Murry microdissected various portions of human atherosclerotic plaques and found that lesions were monoclonal, originating from a SMC in the fibrous cap[8]. After the 1990s and early 2000s, publications in the field no longer investigated clonality; under the assumption that SMCs participate in disease development through dedifferentiation, they focused rather on the relative contribution of SMCs to disease compared to other cell types. However, a couple of very recent publications suggest that interest in clonality will be renewed in the field. Using lineage tracing, a tool that was not

previously available when clonality was last considered, Feil showed that atherosclerotic plaques in the pulse-labeled aorta of ApoE$^{-/-}$/SM22α-CreER^{T2}/R26R-Confetti transgenic mice were monoclonal in origin[51]. Similarly, in 2016, Chappell demonstrated that SMCs were oligoclonal in the neointima of SMMHC-CreER^{T2}/R26R-Confetti mice and in the atherosclerotic plaques of ApoE$^{-/-}$/SMMHC-CreER^{T2}/R26R-Confetti mice[9]. The theories of SMC dedifferentiation and SMC heterogeneity are fundamentally at odds: according to the former, all SMCs have the capacity to participate in vascular disease through a common process, but the latter indicates that there is a predisposed SMC subpopulation that could potentially be therapeutically targeted before the subpopulation participates in disease development.

Most studies of SMCs have been *in vitro* experiments, and because SMCs were surveyed in bulk cultures, it was often ambiguous whether the observations described dedifferentiation or heterogeneity of SMCs. The general consensus has been that two morphologically distinct types of SMCs were observed, either spindle-shaped or epithelioid. Early culture consisted of spindle-shaped, non-proliferative SMCs, and long-term culture contained epithelioid proliferative SMCs. Studies have differed in their explanation of whether this shift depicted the dedifferentiation of all SMCs or the proliferation of a SMC subpopulation that dominated the culture. McCaffrey derived SMCs from the aorta of rats of different ages and determined that both phenotypes were found in all cultures, but younger rat aortas contained more spindle-shaped SMCs while older rat aortas contained more epithelioid SMCs[52]; the significance lay in that other studies have shown older rats to be more prone to intima thickening upon injury to the blood vessel[53,54]. Bochaton-Piallat observed that SMCs cultured from normal uninjured media were mostly spindle-shaped whereas SMCs from neointima predominantly consisted of epithelioid SMCs[55]. Nevertheless, these studies did not effectively elucidate whether the differences in SMCs were due to dedifferentiation or preexisting phenotypes. Moreover, the vast majority of *in vitro* studies of SMCs adopt the practice of expanding and passaging the cells extensively before use, thus introducing the distinct possibility of cell culture artifact confounding the results.

Although the origin of the two types of SMCs is unclear, the phenotypes have been otherwise characterized based on protein expression of general SMC markers. In rat, cow, pig, and human samples, epithelioid SMCs exhibited low positive expression of α-SMA as well as low or negative expression of SMMHC; in contrast, spindle-shaped SMCs expressed high levels of α-SMA and SMMHC[56-60]. These proteins are differentiation markers of SMCs that serve important purposes in contractility, the main function of SMCs. α-SMA is a general marker of SMCs at both early and late stages of development, and SMMHC is a marker of differentiated SMCs. Miano conducted in situ hybridization of mouse embryos at various timepoints, and throughout development, SMMHC was exclusively expressed by SMCs[48].

Additionally, some papers have suggested that epithelioid SMCs may be multipotent, or able to differentiate into a limited number of other cell types. However, opinions have diverged on whether the differentiation potential results from phenotypic plasticity of all SMCs, or whether an inherently immature subpopulation of SMCs resides within the native vessel wall, analogous to progenitor populations that have been discovered in various adult tissues[61]. Most current studies assume that SMCs are a homogenous population that dedifferentiates as

a whole, so recent studies have not compared the different SMC phenotypes as two experimental groups. Nevertheless, when SMC heterogeneity was more intensely investigated, Nicosia showed that epithelioid SMCs demonstrated the potential to promote angiogenesis: epithelioid SMCs differentiated into pericytes and worked in concert with endothelial cells to form microvessels in collagen gel, but spindle-shaped SMCs did not display the same participation in vascular remodeling[62]. Notably, SMCs have also been implicated in vascular calcification through differentiation potential: under high-phosphate conditions, which is a major risk factor in cardiovascular disease, SMCs differentiated into osteoblasts, upregulating expression of osteogenic markers such as alkaline phosphatase, osteocalcin, osteopontin, and Runx2[63]. Vascular calcification was previously believed to be a passive accumulation of calcium in the neointima and media layers, but mounting evidence has indicated that SMCs actively regulate and participate in the deposition of calcium in the vessel wall. Yet, it is unclear whether SMCs in general have the capacity to differentiate into different cell types, or if a subpopulation of SMCs is particularly responsive to changes in the cellular microenvironment as vascular disease progresses.

The most definitive evidence of SMC dedifferentiation would be to deliberately trigger the transition from spindle-shaped to epithelioid SMCs or vice versa in culture. Orlandi harvested SMCs from the aorta of young and old rats to derive mainly epithelioid or spindle-shaped SMCs, respectively. The cultures were then exposed to transforming growth factor-β1 (TGF-β1) and heparin[64]. Heparin and TGF-β1 reduced proliferation, heparin increased α-SMA expression, and TGF-β1 decreased α-SMA expression. These chemical factors generated the same trend in both phenotypes, and no phenotypic switching was observed. Similarly, Seidel described a majority type of SMCs in canine vessels that was incapable of proliferation in culture and thus terminally differentiated[65]. Furthermore, Bochaton-Piallat implanted spindle-shaped or epithelioid SMCs into the carotid artery of rats after injury[66]. Even upon exposure to the *in vivo* environment of an injured vessel, which is the trigger for SMC dedifferentiation, the two populations retained their unique characteristics without switching phenotype.

Thus far, the controversy between dedifferentiation of SMCs or heterogeneity of SMCs has not been resolved. In order to develop effective treatments against vascular disease, it is critical to distinguish whether therapies should target the specific process of dedifferentiation by all SMCs or a specific subpopulation of SMCs that is predisposed to pathogenesis. The latter would encourage preemptive measures to control the subset of SMCs before these cells participate in vascular disease development.

3.2 Materials and Methods

3.2.1 Generation of SMMHC-CreER^{T2}/LoxP-tdTomato Transgenic Mice

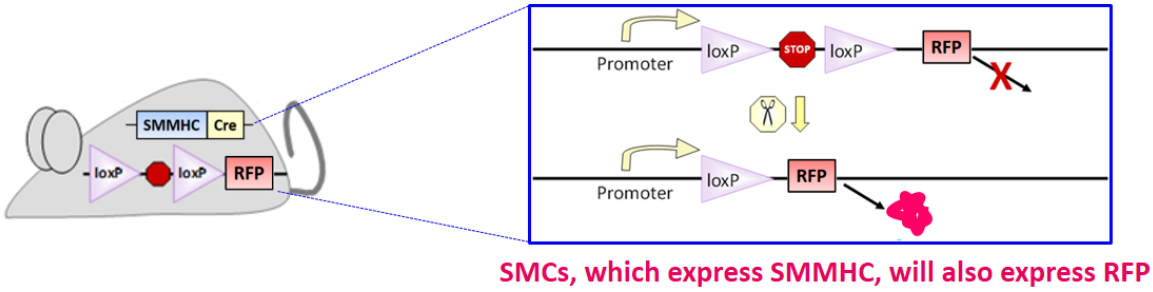

Figure 3.1. Cre/LoxP system for fluorescent labeling of a specific cell type. Cells that express SMMHC also produce Cre recombinase, which excises the floxed stop cassette and allows the downstream RFP to be expressed. Therefore, cells that express SMMHC, or SMCs, will be fluorescently labeled RFP+. Figure is an altered version of a schematic from JAX.

SMMHC-CreER^{T2}/LoxP-tdTomato transgenic mice were generated from breeding SMMHC-CreER^{T2} (JAX, 019079) and Ai9(RCL-tdT) (JAX, 007909) mice. tdTomato, or tandem dimer tomato, is a very bright type of red fluorescent protein (RFP). In SMMHC-CreER^{T2}/LoxP-tdTomato mice, cells that express SMMHC also produce the enzyme Cre recombinase (Figure 3.1). Additionally, SMMHC-CreER^{T2}/LoxP-tdTomato mice contain a floxed, or LoxP-flanked, stop cassette that prevents the downstream RFP from being expressed. Therefore, only cells that express SMMHC and thus Cre recombinase will be able to recombine the LoxP sequences, thereby removing the stop sequence and allowing RFP to be expressed. Because SMMHC is an exclusive SMC marker, RFP+ cells represent fluorescently labeled SMCs.

Furthermore, SMMHC-CreER^{T2}/LoxP-tdTomato transgenic mice are an inducible strain. CreER indicates that the Cre recombinase is fused to an estrogen receptor (ER). Without the presence of tamoxifen, CreER cannot enter the nucleus to recombine the floxed stop; thus, even when SMMHC is expressed, no RFP is expressed. When tamoxifen is present, the tamoxifen binds to the ER and allows CreER to translocate into the nucleus. The primary purpose of an inducible strain is to ensure that cells transiently expressing the protein of interest during development will not be permanently labeled in adult tissue even after the protein is no longer expressed. By injecting tamoxifen prior to experimentation, labeled cells are guaranteed to be cells that expressed the protein during tamoxifen administration. This safeguard is less critical for labeling SMCs using SMMHC, since SMMHC is only expressed by SMCs during development or in adult tissue. Before experiments, SMMHC-CreER^{T2}/LoxP-tdTomato adult mice were given daily intraperitoneal injections of 2 µg of tamoxifen in 100 µL of corn oil for 5 days and used for analysis a week afterward.

Figure 3.2. Verification of specific labeling of SMCs in SMMHC-CreER^{T2}/LoxP-tdTomato transgenic mice. From left to right, the panels show an ear sample from a SMMHC-CreER^{T2}/LoxP-tdTomato mouse, the aorta before detachment from the heart, the aorta after harvest with all three layers of the blood vessel, the aorta after stripping the tunica adventitia layer and endothelial denudation, and a cross-section of the aorta under fluorescence imaging. The ear sample confirmed that fluorescent labeling was restricted to SMCs, as indicated by the structure of a blood vessel network seen under fluorescence. The cross-section of the aorta further verified that RFP+ cells were restricted to the media layer, as expected from labeling of SMCs.

3.2.2 Isolation of Aorta and Enzymatic Digestion to Dissociate Cells

All experimental procedures with mice were approved by the ACUC committee at UC Berkeley and carried out according to institutional guidelines. All efforts were made to minimize the suffering and number of animals used. SMMHC-CreER^{T2}/LoxP-tdTomato mice were euthanized via CO_2 exposure with a CO_2 flow rate of 2 L/min. for 5 min. The mice were then inspected for cessation of movement and respiration for 1 min. A secondary form of euthanasia, cervical dislocation, was performed.

Surgical tools were sterilized using 70% ethanol as well as incubation at 150ºC. The bodies of mice were also sprayed with 70% ethanol for sterilization. To harvest the aorta, incisions were made in the skin and muscle below the diaphragm to access the abdominal cavity. The diaphragm was then punctured, and the thoracic cavity was exposed. The entire aorta was harvested, from the ascending aorta to the abdominal aorta. The aorta was subsequently placed in a dish of cold sterile PBS and stripped of the outer tunica adventitia layer consisting of fibroblasts and connective tissue. The inner endothelial cell layer was dunudated by passing a surgical wire through the vessel back and forth three times. The remaining tunica media layer comprised of smooth muscle cells was cut into short segments and placed in a 1.5 mL microcentrifuge tube filled with cold sterile PBS.

To isolate SMCs from the aorta, the vessel segments were first incubated in a solution of 1 mg/mL collagenase (Sigma, C6885) in 1X PBS containing calcium and magnesium for 10 min. The solution was then discarded, as preliminary digestion of the aorta with collagenase served to minimize cell contamination by other cell types, such as endothelial cells or fibroblasts. Next, the aorta was incubated in a solution of 1 mg/mL collagenase and 0.125 mg/mL elastase (Sigma, E1250) in 1X PBS containing calcium and magnesium[67]. During digestion, the aorta was agitated on an orbital shaker set to 50 rpm at 37ºC for 50 min. The

solution was pipetted up and down to further disperse the digested ECM, spun down at 1500 rpm for 5 min., resuspended, and passed through a cell strainer with 40 µm pores to remove ECM debris and cell clusters.

3.2.3 Single-Cell Contractility Assay

Substrates to assess single-cell contractility were fabricated as previously described[68]. Briefly, silicon wafers were spun-coat at 2000 rpm with 20% dextran in deionized water to a thickness of 1 µm. The wafers were dried at 150ºC and sectioned. The silicon substrates were then coated in 10% amino-dextran and dried overnight. Next, the substrates were stamped with 10 µg/mL GFP-conjugated fibronectin (Thermo Fisher, F13191) for 5 min. using a stamp of 10 µm-thick patterned photoresist on silicon. Polydimethylsiloxane (PDMS) at a ratio of 60:1 for base:crosslinker was spun onto the substrates as a thin film and crosslinked at room temperature for 5 days. A glass coverslip was mechanically adhered to the soft PDMS, and the dextran sacrificial layer was dissolved under gentle agitation in 1X PBS. The result was a soft PDMS layer with a patterned array of 50 µm GFP+ ECM X-shapes. Lastly, the substrates were blocked with 1% Pluronic F-127 (Sigma, P2443) in 1X PBS for 1 h in order to inhibit cell adhesion in the areas surrounding the ECM patterns.

Single cells freshly dissociated from the aorta of SMMHC-CreER^{T2}/LoxP-tdTomato mice were suspended and seeded onto the substrate in cell culture media, Dulbecco's Modified Eagle Medium (DMEM) with 10% fetal bovine serum (FBS) and 1% Penicillin-Streptomycin (Pen-Strep). Media was replaced the next day to wash away the unattached cells. On day 4 in culture, the culture was switched to low-serum culture media (DMEM with 0.5% FBS and 1% Pen-Strep). On day 5, cells were incubated in 1:1000 Hoechst in low-serum media for 10 min. for live-cell nuclear staining. The cells were then washed and cultured in low-serum media for 2 h to allow for recovery from any spontaneous contraction that occurred during media changes. ImageXpress Micro (IXM) equipment was used to automatically image the culture in 3 fluorescent channels in order to visualize the GFP-conjugated ECM patterns, RFP-labeled cells, and Hoechst nuclear stain. 2 µM of endothelin-1 (ET-1, a vasoconstrictor peptide) in 1% acetic acid was added to the existing volume of culture media to a final concentration of 100 nM ET-1 (Sigma, E7764). Contracting cells displaced the soft PDMS and thus changed the fluorescent pattern. Custom image analysis software measured displacement of the patterns by only single cells, as identified by live Hoechst stain, and only RFP+ cells, or SMCs, were selected.

3.2.4 Selection of SMCs during OET Positioning

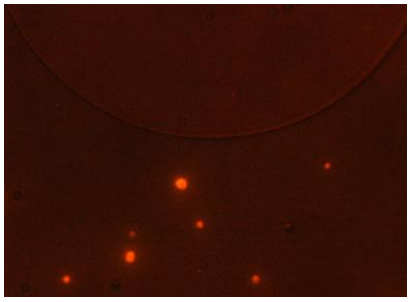

Figure 3.3. SMCs from the aorta of SMMHC-CreER^{T2}/LoxP-tdTomato transgenic mice were selected based on RFP labeling during OET single-cell positioning. RFP+ and RFP-

cells are shown. RFP+ cells appear to be different sizes because they were located at different depths in the fluidic chamber. An RFP+ cell, a SMC, was selected and positioned into the ECM island for subsequent single-cell clonal culture and analysis.

Using OET, single SMCs were positioned into ECM islands. To distinguish between SMCs and other cell types, cells were checked for fluorescence during OET manipulation (Figure 3.3). SMCs from SMMHC-CreER^{T2}/LoxP-tdTomato transgenic mice were labeled RFP+ because they expressed SMMHC. By selecting for SMCs, the efficiency of obtaining single-cell clones of the desired cell type was maximized prior to culture.

3.2.5 Proliferation and Differentiation Assays on Primary Culture of SMCs

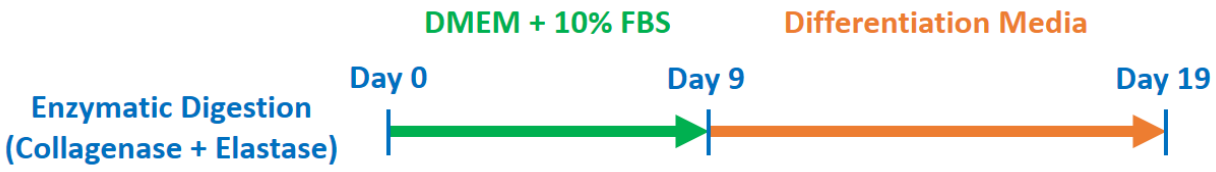

Figure 3.4. Timeline of smooth muscle cell primary culture. SMCs were dissociated from the aorta through enzymatic digestion for primary culture. Live-cell monitoring of expanding single-cell clonal colonies for nine days allowed for comparison of proliferative potential among SMCs. Subsequently, cell cultures were exposed to adipogenic or osteogenic differentiation media for ten days before fixation and staining of lipid droplets or calcified deposits, respectively.

Single-cell analysis of SMCs was critical to determining whether SMCs are heterogeneous. SMCs have been previously implicated in the progression of vascular disease through proliferation into neointima and participation in the ectopic tissue types found in plaques. Therefore, it was important to discern whether single SMCs exhibited different proliferative and differentiation potential (Figure 3.4). Single-cell clones were cultured on a micropatterned substrate of ECM-conjugated islands surrounded by a PEGylated surface. Cell culture media consisted of DMEM with 10% FBS and 1% Pen-Strep. The culture media was replaced every two days. To assess proliferative potential, the cell number within each ECM island was tracked over nine days, and then growth curves were graphed and compared among SMCs. Subsequently, cells were cultured in either adipogenic or osteogenic differentiation media to determine whether SMCs have the capacity to produce lipid droplets or calcified deposits, respectively (Table 3.1). Differentiation media was replaced every other day. After ten days in osteogenic or adipogenic differentiation media, cultures were fixed and stained with Alizarin Red dye or Oil Red O dye.

The stock solution of Alizarin Red dye consisted of 2 g of Alizarin Red powder added to 100 mL of deionized water (DI water) and adjusted to pH 4.1-4.3 using 0.1% NH_4OH. The solution was filtered and stored away from light. For Alizarin Red staining of calcium deposits after osteogenic differentiation, the cell culture was washed with 1X PBS, fixed with 4% paraformaldehyde (PFA) for 10 min., washed with DI water for 5 min., stained with Alizarin Red dye for 15 min., then washed 3 times with 1X PBS for 5 min. per wash. The stained culture was promptly imaged.

The stock solution of Oil Red O dye consisted of 160 mg of Oil Red O powder in 50 mL of isopropanol (IPA). For Oil Red O staining of lipid droplets after adipogenic differentiation, Oil Red O dye was first diluted with DI water at a 3:2 ratio of Oil Red:DI water. The diluted solution was left to sit for 10 min. and then filtered. Next, the cell culture was washed with 1X PBS, fixed with 4% PFA for 10 min., washed with 1X PBS for 5 min., washed with 60% IPA, stained with the diluted Oil Red O solution for 15 min., washed with 60% IPA, and washed 3 times with DI water for 5 min. per wash. The stained culture was promptly imaged.

Adipogenic Differentiation Media	
Reagent	**Concentration**
Dexamethasone	1 µM
Insulin	10 µg/mL
3-isobutylmethylxanthine (IBMX)	0.5 mM
Osteogenic Differentiation Media	
Reagent	**Concentration**
Ascorbic Acid	200 µM
Dexamethasone	0.1 µM
β-glycerophosphate	10 mM

Table 3.1. Chemical components of adipogenic and osteogenic directed differentiation media. The respective reagents for adipogenic or osteogenic differentiation media were added to basic cell culture media (DMEM with 10% FBS and 1% Pen-Strep).

3.3 Results and Discussion

3.3.1 Single-Cell Functional Analysis of Smooth Muscle Cell Contractility

Because the primary purpose of smooth muscle cells is to modulate blood flow through contraction, descriptions of SMC phenotypes have been largely based on contractility. The theory of SMC dedifferentiation was gleaned from the loss of spontaneous contraction from visceral SMCs; dedifferentiation of SMCs is thus defined as the loss of the contractile phenotype. Since then, studies identify the contractile phenotype through the expression of contractile proteins. However, they do not test whether the presence of actin or myosin directly determines functional contractility. To examine the correlation between contractile protein expression and contractile force, single-cell functional analysis of contractility was conducted on SMCs and compared with the expression level of contractile proteins in the same individual SMCs.

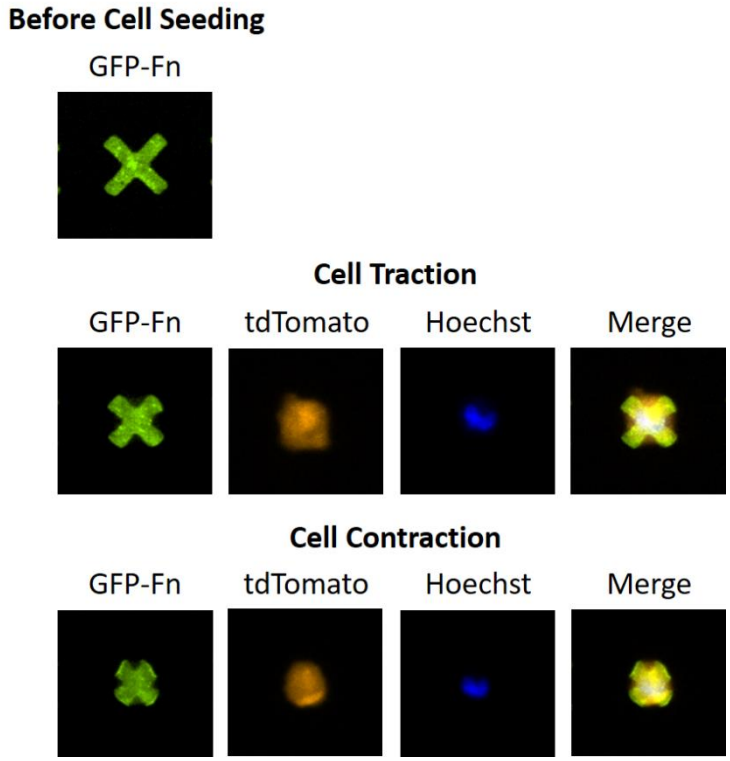

Figure 3.5. Fluorescent images of a single RFP+ cell on a GFP+ ECM pattern exhibiting cell traction after attachment and cell contraction after exposure to endothelin-1. SMCs from the aorta of SMMHC-CreER^{T2}/LoxP-tdTomato transgenic mice were seeded onto 50 μm GFP+ ECM patterns on soft PDMS. The forces of cell traction and contraction were measured through deformation of the four corners of the X-shaped pattern, which would shrink toward the center of the pattern as the cell contracted.

A single-cell contractility assay was used to analyze SMCs: RFP+ SMCs were dissociated from the aorta of SMMHC-CreER^{T2}/LoxP-tdTomato transgenic mice and seeded onto GFP+ ECM X-shaped patterns on a soft PDMS substrate (Figure 3.5). The 50 μm

patterns were designed to fit one cell per pattern. As cells attached and spread, deformation in the four corners of the pattern constituted the force of cell traction. Upon addition of endothelin-1 (ET-1), a potent vasoconstrictor peptide[69], SMCs contracted and caused further deformation of the elastomer, resulting in measurable contractile force. Single SMCs were identified as one RFP+ cell spread on a GFP+ pattern; the presence of a single cell was verified through live Hoechst staining. As a result, contractility of SMCs was analyzed on a single-cell level. Multiple cells on one pattern, a single cell across multiple patterns, or cells that were balled up and not spread out were not included in the analysis. After exposure to ET-1, the cultures rested for 2 h to allow for relaxation of SMCs. The cells were then fixed and immunostained for α-SMA, CNN1, or SMMHC.

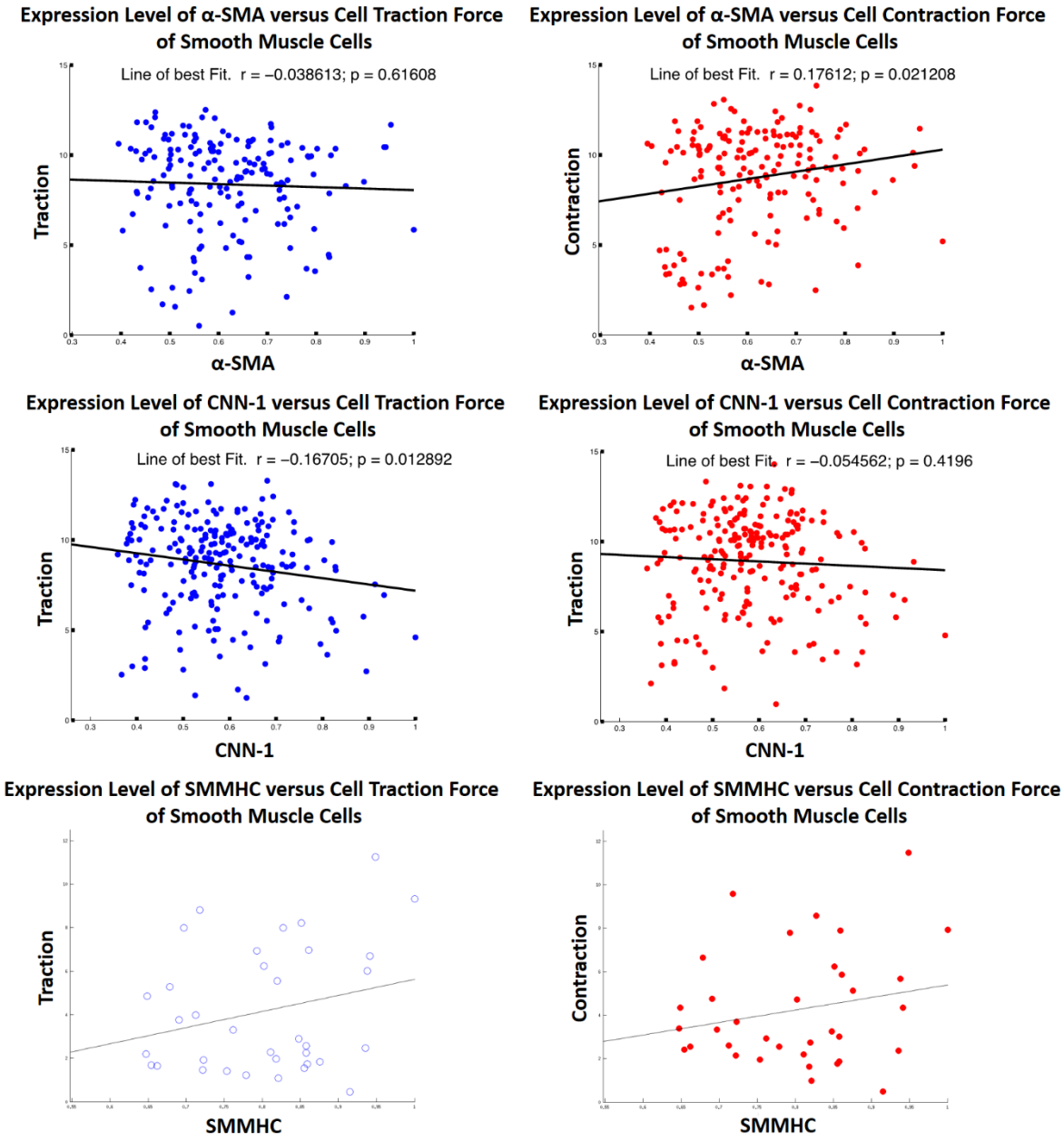

Figure 3.6. Expression level of contractile proteins versus cell traction or contraction force of smooth muscle cells. The force of cell traction or contraction in single SMCs was not dependent on expression level of the contractile proteins α-SMA, CNN1, or SMMHC.

All SMCs were contractile, but the level of contractile force was markedly heterogeneous among SMCs. Surprisingly, the forces of cell traction or contraction did not correlate with the expression of α-SMA, CNN1, or SMMHC, which are identifying markers of SMCs and critical components of the contractile apparatus in SMCs. Consequently, the common reliance of SMC studies on contractile protein expression as an indicator of contractile phenotype may be a misguided assumption, as protein expression does not dictate

functional contractility. The signaling pathway of contractility may be more complex, and mediating enzymes may have a larger influence than production of actin or myosin on contractile force. The phenotypes of SMCs have been frequently characterized as contractile or non-contractile based on the expression of contractile proteins; however, during the progression of vascular disease, the contractility of SMCs is not involved. Rather, the invasive behavioral characteristics of proliferation and differentiation are prominent in the role of SMCs during disease development. Therefore, we conducted single-cell clonal analysis of SMCs to analyze behavioral differences that are more pertinent to the SMCs that participate in vascular disease.

3.3.2 Single-Cell Clonal Analysis of Smooth Muscle Cells using an Optoelectronic Tweezers Platform

Smooth muscle cells have been extensively studied due to their major role in the development of vascular disease. SMCs proliferate and form neointima, blocking the lumen and thus blood flow, and generate ectopic tissue types, such as the calcified and fatty deposits found in atherosclerotic plaques. Studies have predominantly treated SMCs as a homogenous population that responds to perturbation as a whole, but the oligoclonal nature of neointima and plaques contradicts the idea that the dedifferentiation of SMCs is a common process, which would result in distinctly polyclonal outgrowth. If the aberrant proliferation and differentiation of SMCs in vascular disease originates from a limited number of SMCs, a minority subpopulation of phenotypically plastic SMCs may reside within the native vessel wall and respond to vascular injury. Analysis on a single-cell level was essential to determining whether SMCs exhibit heterogeneity. In particular, comparison of proliferative potential and differentiation potential of SMCs on a single-cell level was crucial. As described in Chapter 2, we developed a platform adapting optoelectronic tweezers (OET) to a micropatterned substrate that was designed for clonal culture. OET uses light-induced dielectrophoresis to sort and position particles over a large surface area; for our purposes, it provided a real-time, high-resolution tool for creating an array of single cells. Subsequently, the indexed and isolated clonal colony from each cell was monitored and analyzed over the course of days or weeks. The array of clonal colonies allowed for straightforward comparison of the proliferative or differentiation potential among SMCs on a single-cell level (Figure 3.7).

Another important element of the experimental design was the use of freshly harvested cells from transgenic mice with fluorescently labeled SMCs. Using primary cells without extensive expansion in culture or multiple passages was critical: because SMCs were derived from the native vessel immediately prior to observation, extrapolation of our observations to SMCs in the native vessel was justified. Furthermore, limiting the exposure of cells to culture conditions minimized the possibility of cell culture artifact. Lineage tracing was used to label SMCs through the expression of SMMHC, which is the sole exclusive marker of SMCs. Fluorescent labeling of the cell type of interest also facilitated cell selection during OET positioning. Direct and quantitative comparison of the relative proliferative and differentiation potential of single-cell clones provided evidence of SMC subpopulations and reinforced the theory of SMC heterogeneity.

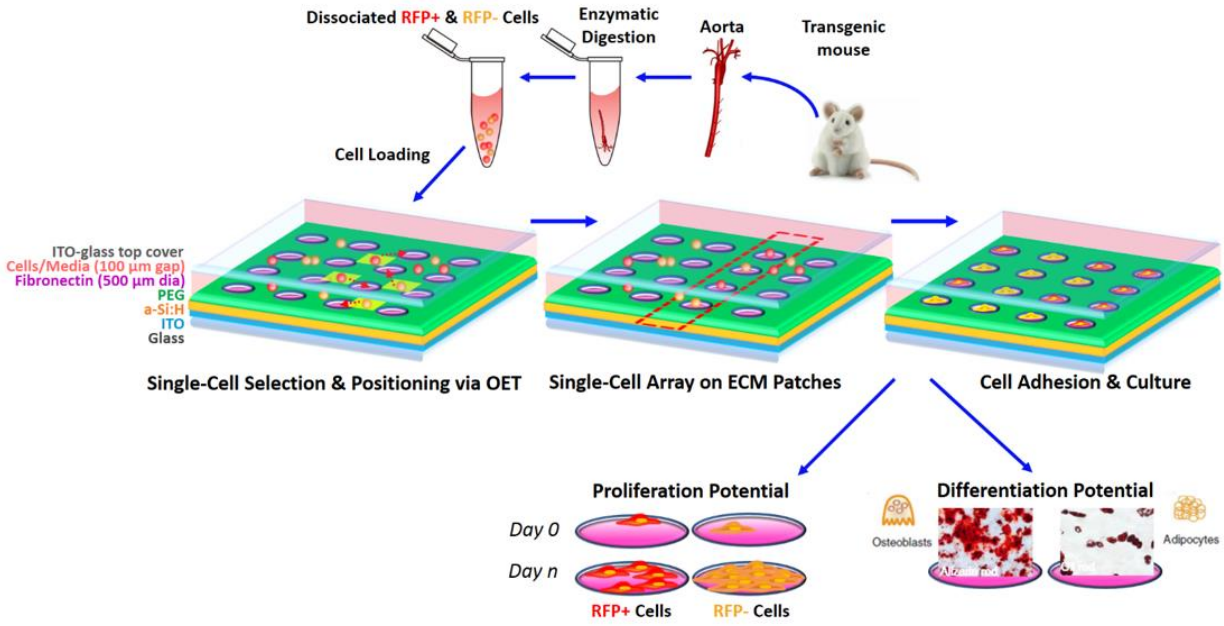

Figure 3.7. Schematic illustrating the workflow of single-cell clonal analysis using an optoelectronic tweezers platform. Fluorescently labeled SMCs harvested from the aorta of SMMHC-CreER^{T2}/LoxP-tdTomato transgenic mice were selected and positioned as a single-cell array using OET. Isolated clonal colonies allowed for comparison of proliferative and differentiation potential among SMCs on a single-cell level.

Conventional cell culture generates data based on bulk analysis, which is often more qualitative than quantitative. For example, proliferation assays typically involve staining of a DNA replication marker, such as expression of Ki67 or incorporation of EdU, which only labels cells that are in certain phases of the cell cycle at the timepoint of fixation or incubation. The indication of proliferation in these techniques is essentially a random sampling, lending a qualitative assessment based on probability. Furthermore, staining for these markers unfortunately requires fixing and thus discontinuing the culture. In contrast, by using OET to position single SMCs on a substrate that was customized for clonal culture, proliferative potential was quantified by imaging and counting the cell number within single-cell clones in live culture over the course of days. Because each ECM island occupied a coordinate in the array, the growth curve of the same clonal colony could be graphed over time and compared to that of other single SMCs.

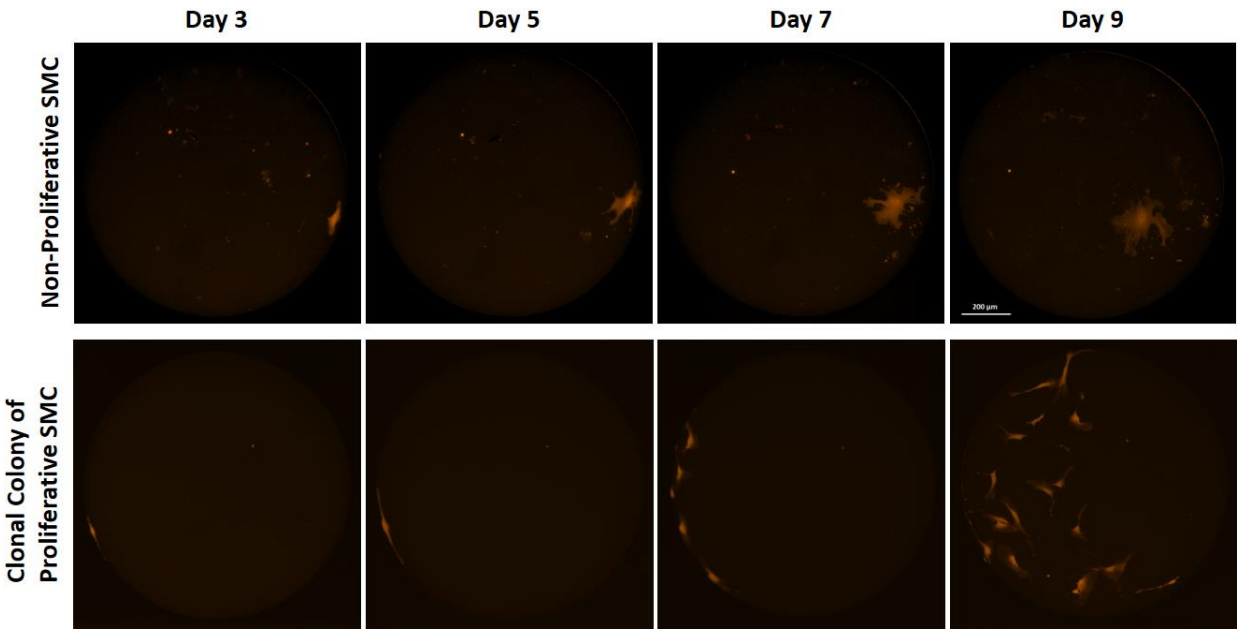

Figure 3.8. Proliferative potential of single smooth muscle cells. Single RFP+ SMCs from the aorta of SMMHC-CreER^{T2}/LoxP-tdTomato transgenic mice on individual 1 mm-diameter ECM islands exhibited differential proliferative potential. Scale bar represents 200 µm.

SMCs, labeled RFP+ as they were harvested from the aorta of SMMHC-CreER^{T2}/LoxP-tdTomato transgenic mice, were arranged in an array with a single SMC per ECM island (Figure 3.8). Generally, the primary cells remained balled up on days 1 and 2 as they recovered after enzymatic digestion from native ECM. By day 3, the cells spread out. On days 5 and 6, a portion of SMCs began to proliferate and migrate within the ECM island. On subsequent days, proliferative SMCs continued to multiply and form clonal colonies. The remainder of SMCs did not proliferate and remained largely stationary in the ECM island. Over time, these non-proliferative SMCs continued to increase in cell surface area. Live-cell monitoring of single SMCs showed two subpopulations of SMCs, proliferative and non-proliferative. Because the SMCs were freshly harvested and immediately used for analysis, these differing behavioral characteristics suggested that SMCs are heterogeneous rather than homogenous within normal vasculature. Dedifferentiation of SMCs may still be occurring, but in contrast to the leading assumption that SMCs are homogenous and all SMCs dedifferentiate upon perturbation, there may be a majority of SMCs that is terminally differentiated while only a subpopulation of SMCs retains the phenotypic plasticity to react with aberrant proliferation.

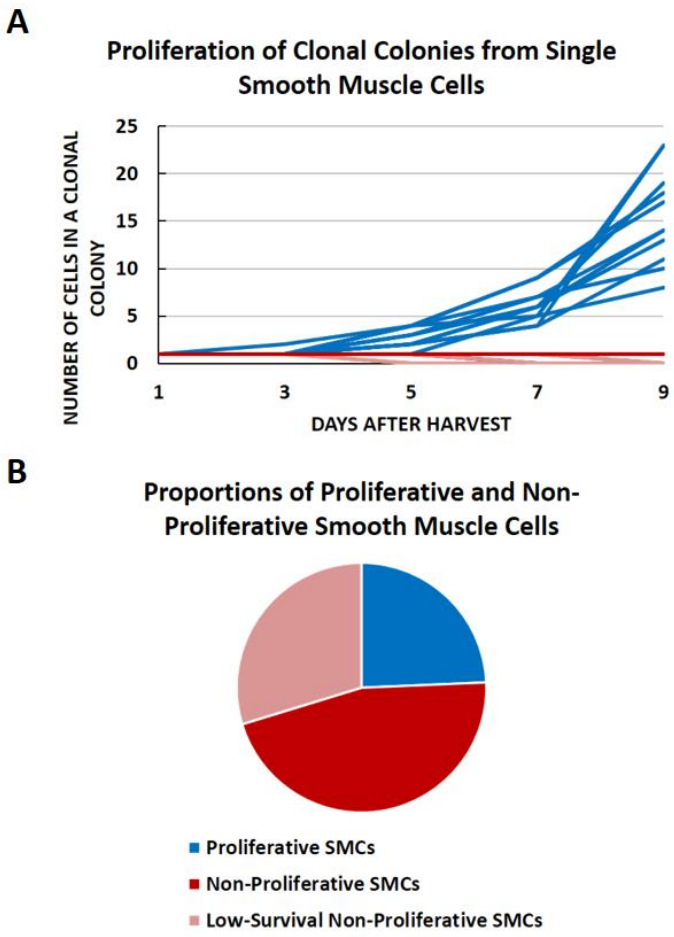

Figure 3.9. Proliferative smooth muscle cells represent a fraction of SMCs. Approximately 24% of all SMCs were proliferative, and 76% were non-proliferative. Additionally, 39% of non-proliferative SMCs, or 29% of all SMCs, exhibited low survival.

Tracking the live-cell behavior of single SMCs demonstrated that two subpopulations of SMCs exist, proliferative and non-proliferative. Furthermore, a portion of non-proliferative SMCs also exhibited low survival: the cells would attach and spread in early culture but subsequently undergo cell death. At approximately day 5 or 6, some SMCs (24%) began to proliferate; the growth of clonal colonies from proliferative SMCs is represented as blue lines in Figure 3.9. Over time, the colonies expanded at an exponential rate. Non-proliferative SMCs that remained single cells throughout culture, denoted by the red line, comprised 76% of all SMCs and 61% of all non-proliferative SMCs. The pink lines signify non-proliferative SMCs with low survival: 39% of non-proliferative SMCs, or 29% of all SMCs, underwent cell death in spite of attaching, spreading, and surviving earlier in culture. Non-proliferative SMCs consistently displayed low activity, without proliferation or migration. Consequently, non-proliferative SMCs seemed to be terminally differentiated. On the other hand, proliferative SMCs only represented a fraction of all SMCs but launched a robust proliferative response. Taken together, these observations indicated that upon injury to a blood vessel, the majority of SMCs may lack the capacity to respond, but a fraction of SMCs account for the well-

documented pathogenesis of SMCs as they proliferate and migrate to form a neointimal layer during disease development.

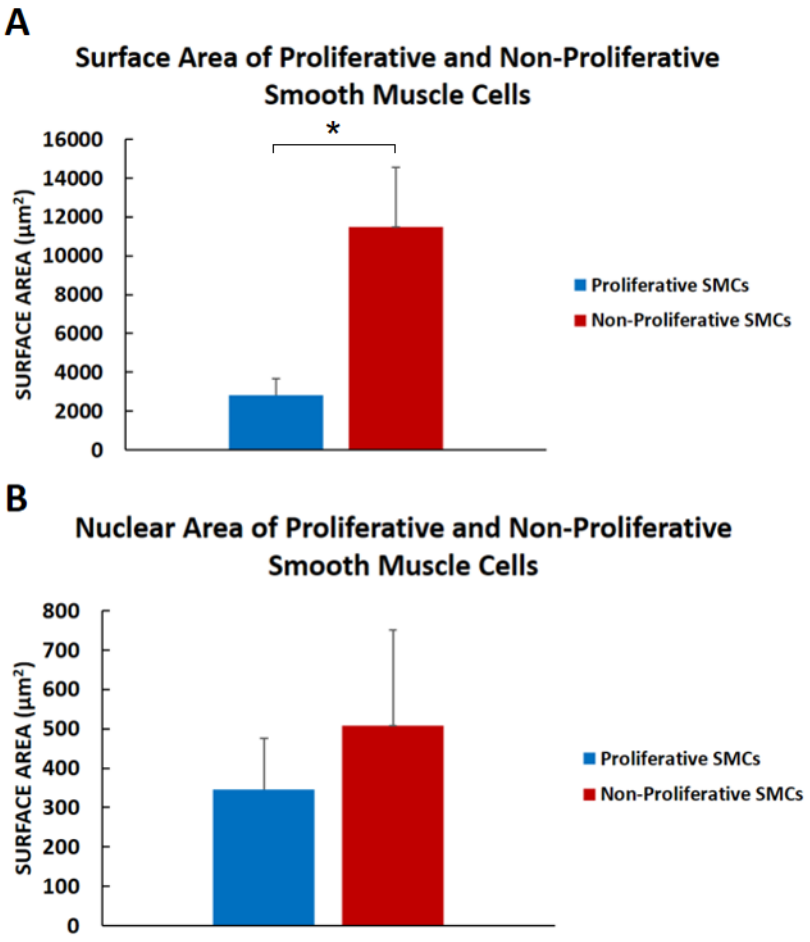

Figure 3.10. Smooth muscle cell subpopulations can be distinguished through cell spreading but not nuclear size. Non-proliferative SMCs displayed a significantly higher cell surface area than proliferative SMCs on day 7 in primary culture. No significant difference in nuclear area was observed between proliferative and non-proliferative SMCs.

As can be qualitatively observed in Figure 3.8, proliferative and non-proliferative SMCs presented different degrees of cell spreading. Figure 3.10a quantifies the comparison in cell surface area of proliferative and non-proliferative SMCs on day 7 in primary culture. Non-proliferative SMCs exhibited an average surface area of 11473 μm^2 while proliferative SMCs exhibited an average surface area of 2828 μm^2. We tested whether the difference was statistically significant: an f-test determined that the variances of the two populations were not equal, and a t-test for populations with unequal variances was performed. From the two-tailed t-test, the t-statistic (7.885) was found to be greater than the critical value of t (2.365). Therefore, we rejected the null hypothesis and determined that the difference in cell surface area between proliferative and non-proliferative SMCs was statistically significant. Because non-proliferative SMCs exhibited significantly higher spreading than proliferative SMCs, cell

surface area offers a physical characteristic to distinguish between SMC subpopulations of different behavioral characteristics.

Given that proliferative and non-proliferative SMCs displayed a disparity in cell surface area, we examined whether the larger cell spreading correlated with larger nuclei as well. As shown in Figure 3.10b, nuclear size was not significantly different between proliferative and non-proliferative SMCs (on average 509 and 345 μm^2, respectively) to discriminate between the two subpopulations.

3.3.3 Single-Cell Analysis of the Differentiation Potential of Smooth Muscle Cells

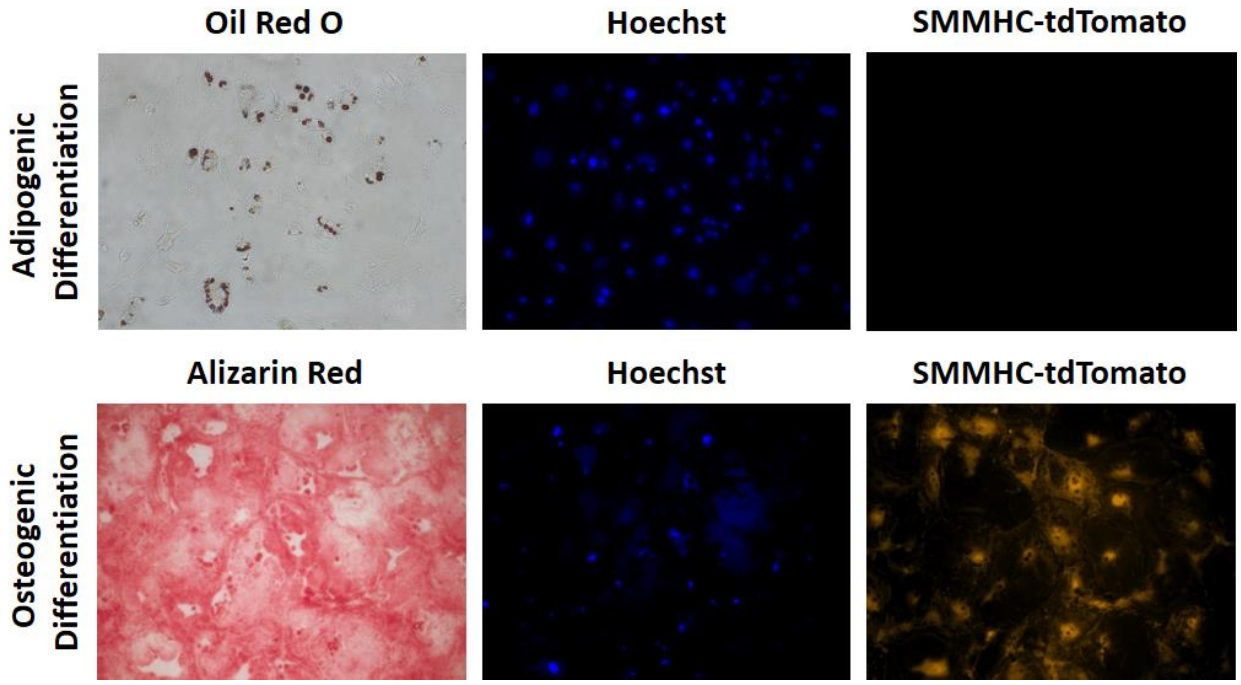

Figure 3.11. Bulk differentiation of cells from the aorta of SMMHC-CreER^{T2}/LoxP-tdTomato transgenic mice. Positive Oil Red O staining of lipid droplets was observed near RFP- cells. Positive Alizarin Red staining of calcified deposits was observed near RFP+ cells.

Ectopic tissue types found in diseased vessels, such as lipid accumulation and calcium-phosphate deposition, compromise the structural integrity of the blood vessel wall and thus impair the ability of the vessel network to supply nutrients to downstream organ systems. Vascular calcification was previously considered to be a passive precipitation of minerals in necrotic tissue. However, recent studies have shown that SMCs may actively regulate and participate in calcium deposition[70]. For example, high-phosphate conditions in culture, which resemble the hyperphosphatemia in blood that is a major risk factor in cardiovascular disease, promoted osteogenic differentiation in SMCs. SMCs that developed matrix mineralization also upregulated expression of osteogenic markers such as Runx2, osteocalcin, osteopontin, and alkaline phosphatase[71,72]. To verify the differentiation potential of SMCs, cells derived from the aorta of SMMHC-CreER^{T2}/LoxP-tdTomato transgenic mice were exposed to osteogenic differentiation media. Components of the osteogenic differentiation media were β-

glycerophosphate, dexamethasone, and ascorbic acid; all three reagents have been implicated in promoting osteogenesis in SMCs[73]. Subsequently, the cells were fixed and stained with Alizarin Red dye. Positive red staining of calcium deposits was observed in areas with primarily SMCs and some RFP- cells, which represented other cell types (Figure 3.11). However, because the cell culture was a heterogeneous bulk culture, it was problematic to assert that a specific cell type was responsible for the widespread mineralization. Moreover, recent studies characterize SMCs as a homogenous cell type, but attributing vascular calcification to SMCs in general discounts the possibility that a phenotypically plastic subpopulation of SMCs resides within the native vessel wall and responds to perturbation during disease development.

Aggregation of lipids in the vessel wall is the first step to the development of atherosclerotic plaques. The main cell type to interact with lipids is macrophages, which uptake lipids and transform into foam cells, but studies have suggested that SMCs can uptake lipids as well[74,75]. Given the potential of SMCs to differentiate into osteoblasts, we tested whether SMCs could differentiate into adipocytes as well. SMCs from the aorta of SMMHC-CreER^{T2}/LoxP-tdTomato transgenic mice were exposed to adipogenic differentiation media, which consisted of reagents known to promote adipogenesis: insulin, dexamethasone, and IBMX[76]. Dexamethasone is a component of both osteogenic and adipogenic differentiation media as it has been shown to promote osteogenesis at lower concentrations and adipogenesis at higher concentrations[77,78]. Subsequently, the cells were fixed and stained with Oil Red O dye. Positive staining of lipid droplets was observed in an area of the culture dish without RFP+ cells, or SMCs. It appeared that SMCs were capable of osteogenesis but not adipogenesis, and a different cell type had the capacity to undergo adipogenic differentiation.

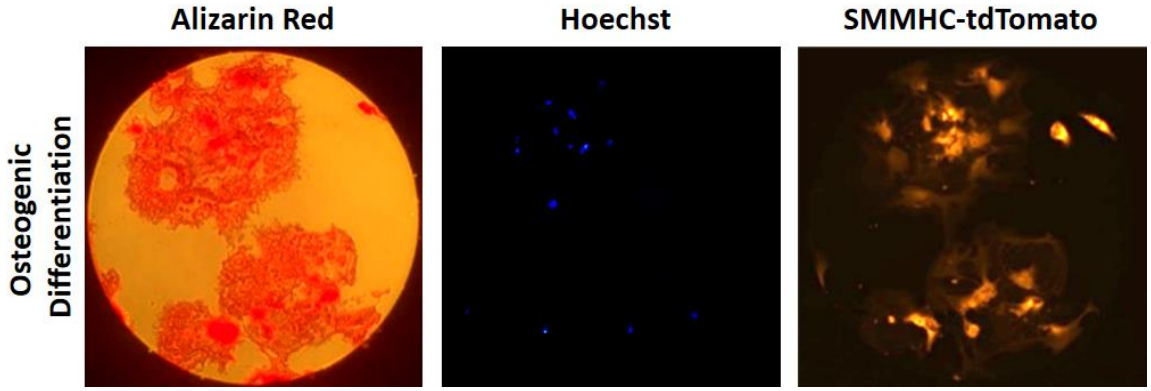

Figure 3.12. Osteogenic differentiation of a clonal colony derived from a single proliferative smooth muscle cell. Proliferative SMCs were able to undergo osteogenic differentiation and generate calcified deposits that were stained positive with Alizarin Red dye.

Conventional cell culture indicated that SMCs were capable of differentiating into osteoblasts but not adipocytes. Other studies using bulk culture methods have similarly observed that SMCs underwent osteogenic differentiation; these studies treated SMCs as a homogenous population and concluded that SMCs in general responded to high-phosphate conditions. Those experiments did not consider that SMCs may be heterogeneous, and a specific subpopulation of SMCs may retain the capacity to differentiate when exposed to the

changing environment of developing plaques. In Figure 3.11, although we applied a strict lineage tracing technique that guaranteed the identification of SMCs through RFP labeling, bulk culture was still a handicap to discerning whether SMCs are heterogeneous. Although SMMHC is an exclusive marker of SMCs, distinguishing between RFP+ and RFP- cells may not be enough; positive labeling indicates the expression of a specific protein, but there may be underlying varying levels of protein expression that translate into behaviorally different phenotypes. Given that SMCs exhibited differential proliferative potential on a single-cell level, we examined whether proliferative and non-proliferative SMCs also showed dissimilar differentiation potential. In order to correlate differentiation potential with proliferative potential, single SMCs were initially cultured in regular culture media, and we observed which SMCs were proliferative. Next, clonal colonies of proliferative SMCs and single non-proliferative SMCs were cultured in osteogenic or adipogenic differentiation media. Proliferative SMCs consistently stained positive for heavy calcium deposits, as seen in Figure 3.12, but never developed lipid droplets. Non-proliferative SMCs were unable to undergo adipogenic or osteogenic differentiation. As a result, a specific subpopulation of SMCs may be responsible for both the aggregation of SMCs in neointima formation and the buildup of ectopic calcified deposits in plaque formation. Additionally, while SMCs have been shown to uptake lipids, they are not capable of differentiating into adipocytes to further promote the progression of fatty buildup in vascular disease.

3.4 Conclusion

Single-cell analysis of functional contractility showed that although all SMCs were contractile, the level of contractile force was heterogeneous among SMCs. Unexpectedly, the expression level of contractile proteins, which are frequently used to characterize SMCs as the contractile phenotype, did not correlate with the level of contractile force exhibited by single SMCs. Furthermore, single-cell clonal analysis revealed two SMC subpopulations with behavioral differences. By fabricating a platform specialized to clonal culture and optimizing single-cell seeding efficiency through OET positioning, we tracked the live-cell behavior of single SMCs over time. SMCs showed distinct heterogeneity: SMCs that were proliferative also had the capacity to undergo osteogenic differentiation and form calcium deposits, and SMCs that were non-proliferative were unable to differentiate into osteoblasts or adipocytes. As a result, the majority of SMCs appears to be the non-proliferative and non-migratory SMCs that serve the primary purpose of regulating blood flow; however, a minority subpopulation of SMCs exists that retains the ability to proliferate and migrate to form neointima as well as contribute to vascular calcification.

Chapter 4: Single-Cell Protein Expression Analysis of Smooth Muscle Cells

4.1 Introduction

4.1.1 Protein Markers of Smooth Muscle Cells

The thickest layer of the blood vessel wall is the tunica media, which contains multiple layers of smooth muscle cells. The primary purpose of smooth muscle cells is to control blood flow through contraction; thus, the identifying protein markers that characterize SMCs are smooth muscle isoforms of the contractile apparatus[3]. Actin and myosin are critical to the structure and function of the contractile apparatus. Alpha smooth muscle actin (α-SMA) is the earliest protein expressed during the development of SMCs[79]. As a result, α-SMA is a broadly useful marker for labeling SMCs[44]. However, studies have become overly reliant on using α-SMA to identify SMCs. Other cell types, such as myofibroblasts and macrophages, can also express α-SMA[13,80]. α-SMA should be used in concert with other SMC markers to definitively detect SMCs. Calponin-1 (CNN1), which binds to actin to regulate contraction, is expressed later in the development of SMCs[45]. CNN1 is also a nonspecific marker of SMCs, as it can be expressed in cardiomyocytes and tumor cells as well[46,47]. Smooth muscle myosin heavy chain (SMMHC) is a major contractile protein that is the most reliable marker for SMCs[81,82]. SMMHC has been proven to not be expressed by any other cell type during development or in adult tissue[48].

Because SMMHC is an exclusive marker of SMCs, fluorescently labeled cells derived from SMMHC-CreER^{T2}/LoxP-tdTomato transgenic mice can be positively identified as SMCs. However, lineage tracing does not account for the possibility that the binary nature of fluorescence, negative or positive, masks differential levels of protein expression underlying positive fluorescence. A cell type may include different subpopulations that express the same cell type markers at varying levels, leading to different cell behavior. Common techniques that process cell cultures in bulk would further conceal these differences with averaging effects; for example, conventional Western blotting pools the lysed contents of thousands of cells. Conventional Western blotting of multiple proteins also presents another major issue: analyzing a population for multiple protein markers may lead to the assumption that the population as a whole expresses those proteins at those levels. However, the reality may be that separate subpopulations express those proteins at drastically different levels, but the expression levels become a blended parameter as a Western blot band for the entire population. Therefore, we used lineage tracing in concert with single-cell Western blotting to provide protein analysis on a single-cell level. Furthermore, single-cell Western blotting allowed us to probe each SMC for several SMC markers: the level of protein expression from one marker was directly associated with the levels of protein expression from other markers within every single cell.

4.2 Materials and Methods

4.2.1 Immunostaining

Cells were fixed with 4% paraformaldehyde (PFA) for 10 min., then washed 3 times with 1X PBS for 5 min. each. Next, the cell membranes were permeabilized through incubation in 0.5% Triton-X 100 for 10 min. and washed with 1X PBS. The cultures were subsequently immersed in 0.1% bovine serum albumin (BSA) for 30 min. for blocking of nonspecific binding. The cells were incubated in primary antibody at 4ºC overnight. The next day, they were washed 3 times in 1X PBS for 5 min. each and left in species-specific fluorescence-conjugated secondary antibody for 45 min. After thorough washes in 1X PBS, the cultures were incubated in Hoechst nuclear stain for 10 min. and washed again. The stained substrates were then mounted, sealed, and imaged. ImageXpress Micro (IXM) equipment was used for automated imaging in order to control conditions such as background noise and exposure time, which could influence quantification of immunostaining intensity. Fluorescence intensity was quantified using ImageJ.

Antibody	Company	Catalog Number
SMMHC	Biomedical Technologies	BT-562
CNN1	Abcam	ab46794
α-SMA	Abcam	ab7817

Table 4.1. Antibody information for immunostaining.

4.2.2 Single-Cell Western Blotting

Single cells, freshly dissociated from the aorta of SMMHC-CreER^{T2}/LoxP-tdTomato transgenic mice, were suspended in 1X PBS, pipetted onto a 30 μm-thick photoactive polyacrylamide (PA) gel on a glass slide, and allowed to settle into an array of 100 μm microwells. The cells were lysed and analyzed as previously described[83]. Briefly, the gel was imaged under brightfield for future reference of which wells contained only one cell as well as imaged under fluorescence to note which wells contained RFP+ cells. The gel was subsequently immersed in lysis buffer, and the cells were lysed for 40 s. Polyacrylamide gel electrophoresis (PAGE) was run for 50 s to separate proteins by molecular mass. The proteins were then immobilized in the gel through photoactivated blotting: the UV initiated a reaction to covalently bond proteins to the PA gel, thus retaining high local protein concentrations and maintaining protein separation. The gel was incubated in primary antibodies and then fluorescence-conjugated secondary antibodies. The intensity profile of each band was analyzed using ImageJ.

Antibody	Company	Catalog Number
SMMHC	Abcam	ab683
CNN1	Abcam	ab46794
α-SMA	Abcam	ab7817

Table 4.2. Antibody information for single-cell Western blotting.

4.3 Results and Discussion

4.3.1 Single-Cell Protein Expression Analysis of Smooth Muscle Cells from the Native Vessel

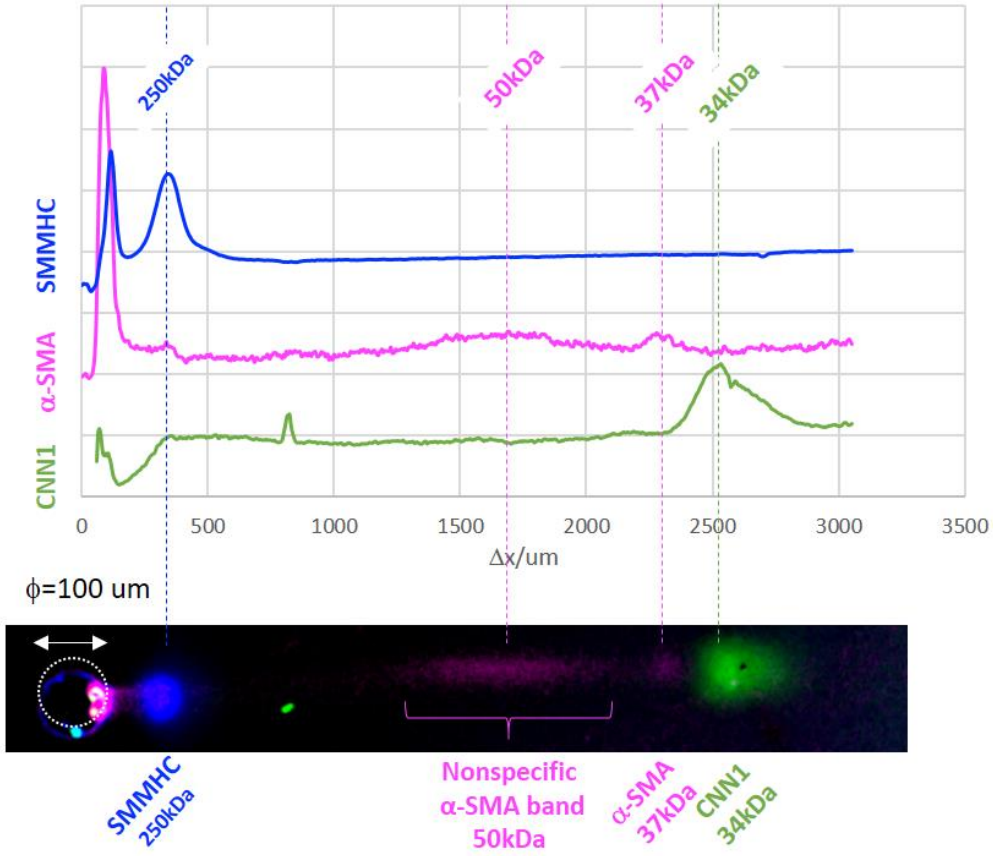

Figure 4.1. Single-cell Western blotting intensity profile of smooth muscle cell markers. Each RFP+ cell, or a single SMC, was probed for its protein expression levels of SMMHC (250 kDa), α-SMA (37 kDa), and CNN1 (34 kDa).

Single-cell Western blotting provides quantitative data on protein expression at a single-cell resolution. For our purposes, it offered the unique ability to analyze and quantify the protein expression levels of SMCs that were freshly dissociated from native ECM. Thus, we could compare SMCs in primary culture to SMCs harvested from the blood vessel wall that had not been exposed to cell culture conditions. Single cells were derived from the aorta of a SMMHC-CreER^{T2}/LoxP-tdTomato mouse and settled into 100 μm-diameter microwells. The entire gel was imaged for future reference in order to rule out any wells that did not contain a single RFP+ cell, or SMC. After lysing the cells and running the gel, the gel was immunostained with antibodies for SMMHC, CNN1, and α-SMA; each marker was imaged at a different wavelength. The expression levels of SMMHC, CNN1, and α-SMA from each SMC were quantified. An intensity profile was taken along the lane to measure the expression level of each protein and to ensure that each protein was detected at the correct molecular weight.

As expected, SMMHC was detected at 250 kDa, CNN1 was detected at 34 kDa, and α-SMA was detected at 37 kDa. α-SMA contained a separate nonspecific band at 50 kDa that was ruled out, as the smear was not located at the correct molecular weight. The nature of Western blotting allowed for verification that the correct protein was probed and quantified at the appropriate molecular weight, and background noise from a nonspecific band would not be erroneously included in the quantification. Because SMCs were dissociated from native ECM and immediately analyzed, the protein expression of SMCs from the natural *in vivo* environment was assessed without any chance of cell culture conditions influencing expression levels.

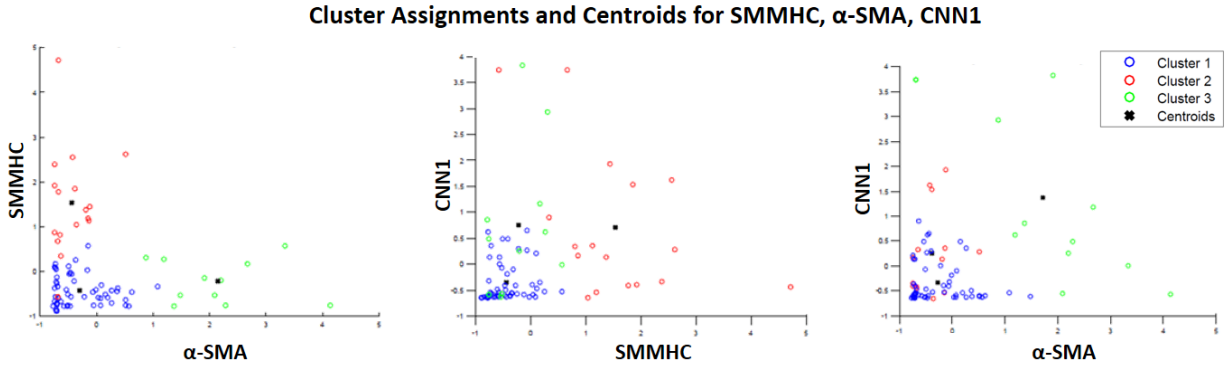

Figure 4.2. 2D projections of 3D plot graphing SMMHC, α-SMA, CNN1. The protein expression profile of each SMC for SMMHC, CNN1, and α-SMA were plotted and clustered using the k-means method. The relationship between SMMHC and α-SMA was determined to be the most influential factor in clustering.

The expression levels of SMMHC, CNN1, and α-SMA for each SMC was quantified using the intensity profile of each Western blot band. Next, the values were standardized to ensure that the range of values for each marker would be identical; otherwise, a particular marker may carry inherent weight and skew the results of clustering. For example, the average of all α-SMA values was subtracted from each α-SMA value, then divided by the standard deviation of all α-SMA values. The final values were then graphed on a 3D plot, in which each point signified an individual SMC. After using the k-means method for clustering with k=3, clusters were delineated in different colors, and the location of centroids was marked as well. The relationship between SMMHC and α-SMA was determined to be the dominant factor in determining cell clusters.

4.3.2 Single-Cell Protein Expression Analysis of Smooth Muscle Cells from Primary Culture of Single SMCs

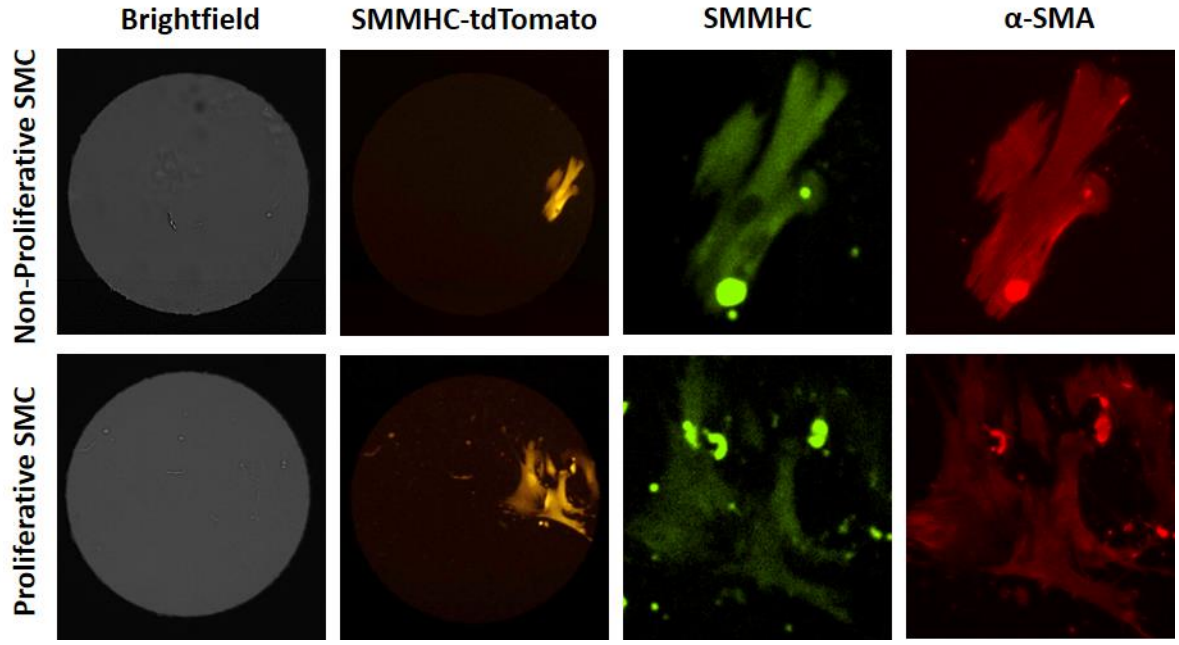

Figure 4.3. Immunostained single-cell clones of proliferative and non-proliferative smooth muscle cells on day 5 in primary culture. Single SMCs were cultured on 500 μm-diameter islands and immunostained for SMMHC and α-SMA on day 5 in culture in order to correlate behavioral differences with differences in protein expression.

Single-cell Western blotting showed that the relationship between SMMHC and α-SMA was the most influential to defining clusters in the population of SMCs from native tissue. The next step was to determine whether there were differences in the relationship between SMMHC and α-SMA for proliferative and non-proliferative SMCs in primary culture. In other words, we tested whether those subpopulations based on behavioral differences could be distinguished through clustering of protein expression profiles.

To compare the protein expression levels of the two SMC subpopulations that exhibited different potential for proliferation and differentiation, single non-proliferative SMCs and clonal colonies of proliferative SMCs were fixed on day 5 in primary culture and immunostained for SMMHC and α-SMA (Figure 4.3). Day 5 was chosen as an early timepoint where minimal change in protein expression will have occurred in culture after recovering from enzymatic digestion; additionally, the majority of SMCs that have the capacity to proliferate will have proliferated by day 5. Overall, proliferative SMCs appeared to have lower SMMHC and α-SMA expression than non-proliferative SMCs. The intensity of immunostaining for each SMC was quantified and plotted to visualize the distribution in the SMC population (Figure 4.4).

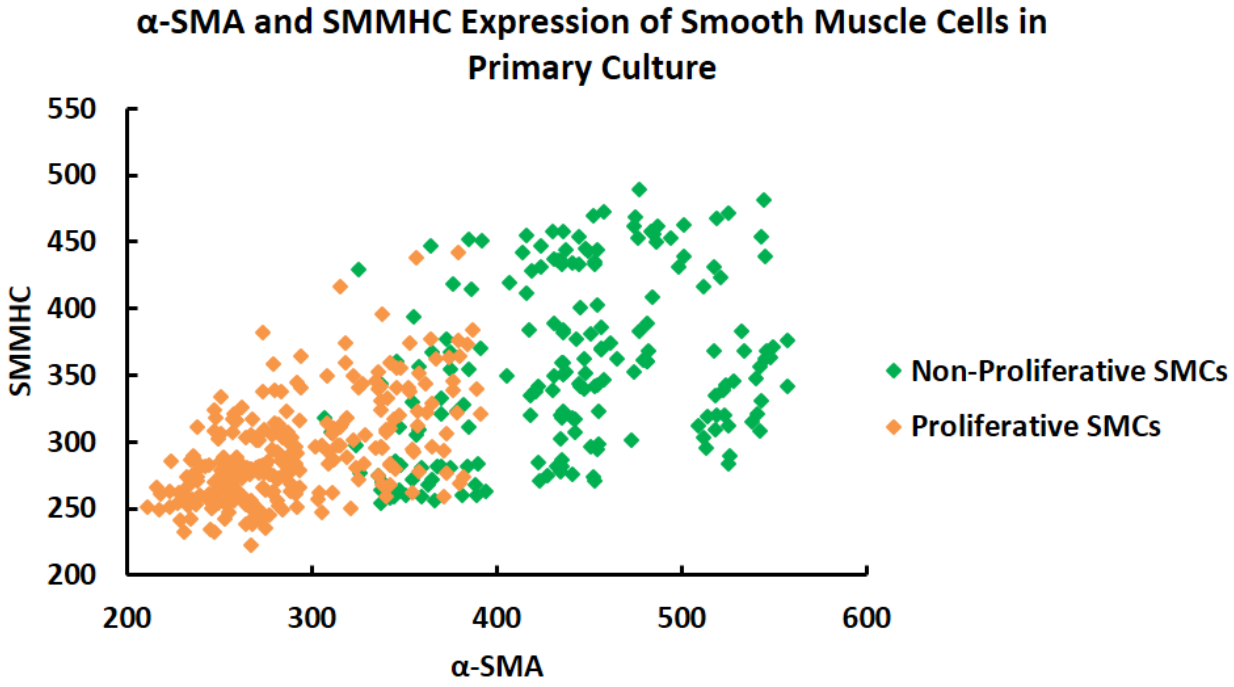

Figure 4.4. α-SMA and SMMHC expression profiles of proliferative and non-proliferative SMCs on day 5 in primary culture. Single non-proliferative SMCs and clonal colonies of proliferative SMCs were co-stained for α-SMA and SMMHC. Protein expression level was plotted, and differential proliferative potential was color-coded.

SMC subpopulations based on proliferative potential are marked in different colors. Non-proliferative SMCs consistently exhibited higher α-SMA levels than proliferative SMCs, with average pixel intensities of 439 versus 290, respectively. The range of values in α-SMA expression for each subpopulation was fairly distinct as well. Proliferative SMCs expressed somewhat lower levels of SMMHC than non-proliferative SMCs, with average pixel intensities of 292 and 356, respectively. More overlap in range was observed in SMMHC expression between the two subpopulations. Proliferative SMCs tended to skew more heavily toward lower SMMHC and α-SMA compared to the more even distribution of both markers observed in non-proliferative SMCs. Notably, the area of overlap in α-SMA expression between the subpopulations may be a result of some proliferative SMCs that had yet to proliferate by day 5 and were thus marked as non-proliferative; although most proliferative SMCs will have proliferated by day 5, a small fraction of SMCs may not have proliferated yet at the time of fixation but would have proliferated a day or so later. However, to minimize arguable cell culture artifact influencing the protein expression profile, cells were fixed at an earlier timepoint at which point most proliferation had begun to occur.

SMCs in the tunica media are known to express SMMHC and α-SMA. Nevertheless, the level of expression may be heterogeneous among SMCs and result in different phenotypes. The plot in Figure 4.4 suggests that the SMC subpopulations with differences in proliferation and differentiation also differ in levels of protein expression. Although lineage tracing is a

useful tool for identifying SMCs in general, extensive analysis on a single-cell level is required to discern subpopulations among SMCs.

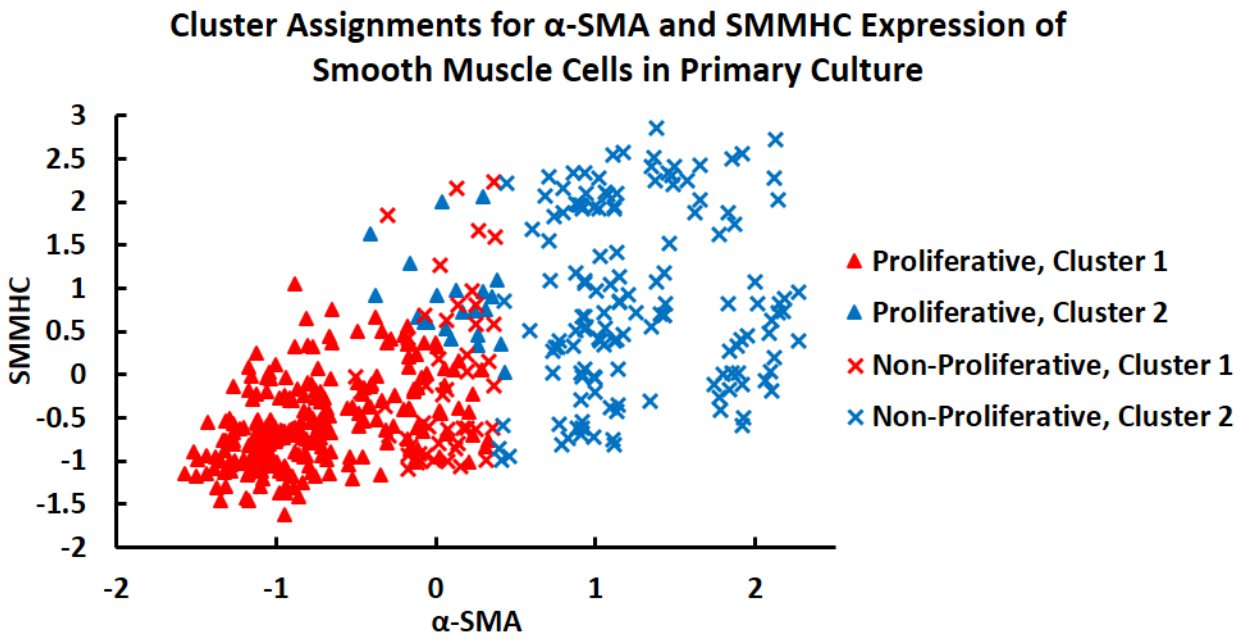

Figure 4.5. Comparison of proliferative and non-proliferative SMC subpopulations with clusters determined by the k-means method. The protein expression profiles of all SMCs were combined and clustered based on the k-means method, as demarcated by red and blue. Grouping based on proliferative potential was then overlaid as different marker shapes in order to assess how closely the subpopulations matched.

Two subpopulations of SMCs were identified thus far through disparate behavior and protein expression. To determine whether these subpopulations could be recognized as statistically distinct, the k-means method of clustering was applied to all SMCs, with proliferative and non-proliferative SMCs combined as one group. As before, the range of values for α-SMA and SMMHC was standardized to ensure that neither marker would carry inherent weight and skew the results of clustering. The clusters determined by the k-means method are shown as different colors in Figure 4.5. The subpopulations of proliferative and non-proliferative SMCs are demarcated by different marker shapes. The k-means clusters very closely matched the SMC subpopulations based on behavior: cluster 1 contained nearly all proliferative SMCs, and cluster 2 contained nearly all non-proliferative SMCs. As mentioned previously, the exceptions that fell along the boundary may be partially ascribed to proliferative SMCs that had not yet begun to multiply by day 5 and were thus labeled non-proliferative. The close similarity between the SMCs grouped by proliferative potential and k-means clusters of protein expression validated the legitimacy of SMC subpopulations that differ on phenotypic and protein expression levels.

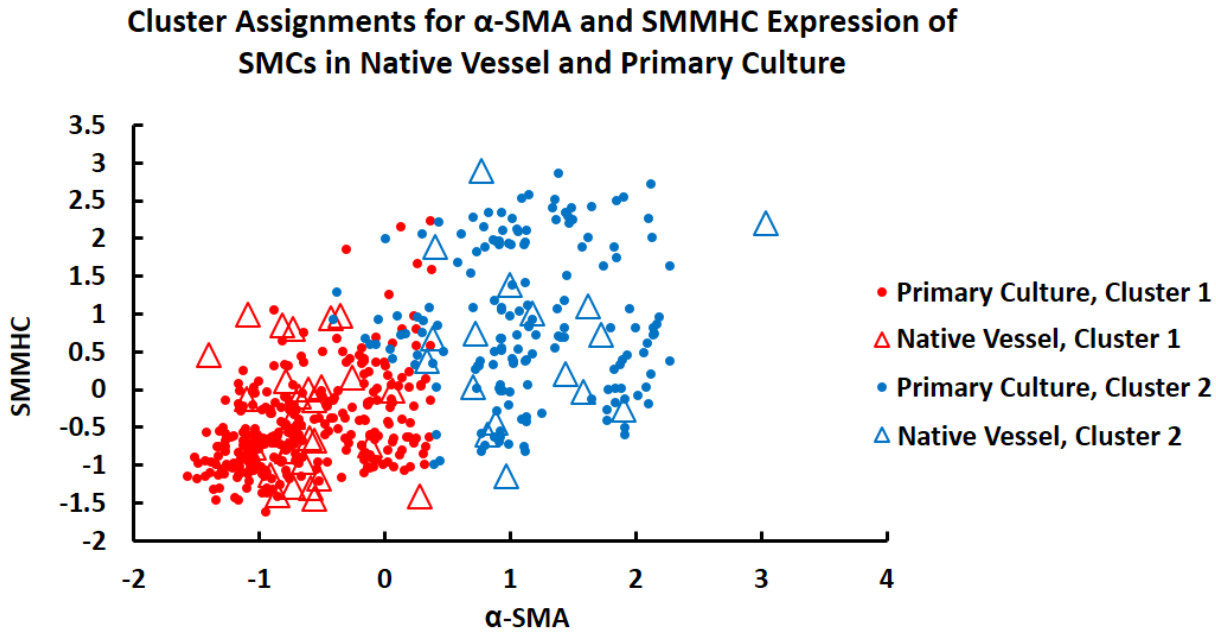

Figure 4.6. Comparison of clusters found in SMCs from native vessel and clusters in SMCs from primary culture. Protein expression profiles from single-cell Western blotting of SMCs from the native vessel were clustered by k-means method and overlaid with the clusters from the protein expression profiles of SMCs in primary culture.

Through single-cell Western blotting of SMCs from the native blood vessel, the relationship between SMMHC and α-SMA was determined to be the most influential factor in the 3D plot of SMMHC, α-SMA, and CNN1. Thus, the data was re-plot as a 2D plot of SMMHC and α-SMA, and the data points, represented by triangles, were clustered using the k-means method, with the clusters in red and blue (Figure 4.6). These clusters were then compared to the clusters from immunostaining of SMCs in primary culture, as previously seen in Figure 4.5. The clusters matched exactly, thus confirming the existence of two SMC subpopulations with different protein expression profiles both in the normal uninjured vessel as well as upon perturbation when dissociated in culture. Therefore, the behavioral differences in proliferation and differentiation and the differences in protein expression were not due to cell culture conditions. Two subpopulations of SMCs that are inherently different exist within the normal blood vessel wall. When the vessel wall becomes disrupted during disease progression, the minority subpopulation of SMCs likely drives the response of proliferating into the lumen and forming ectopic calcified deposits.

4.4 Conclusion

Single-cell Western blotting provided quantitative analysis of protein expression in individual SMCs: the protein expression profile of SMMHC, CNN1, and α-SMA was plotted for each SMC. Through k-means clustering, we observed that the relationship between SMMHC and α-SMA was dominant among the SMC markers in discerning subpopulations. Subsequently, the immunostaining intensity of SMMHC and α-SMA for SMCs in primary culture was quantified and clustered, and given the advantage of clonal culture, we could

correlate protein expression with behavioral analysis of proliferative potential. Among the SMCs in primary culture, the clusters from protein expression very closely matched the subpopulations characterized by proliferative potential. Additionally, the clusters from single-cell Western blotting matched the clusters from primary culture exactly. Because the SMCs from single-cell Western blotting were dissociated from the native vessel immediately prior to lysis and analysis, we could conclude that the subpopulations of SMCs with different potential for proliferation and differentiation, as observed in primary culture, were reflective of existing SMC heterogeneity within the normal vessel wall.

Chapter 5: Conclusion

The study of smooth muscle cells has become a field of its own due to the incrimination of SMCs in the pathogenesis of various fatal diseases, including atherosclerosis and cancer. Dysfunction of the network of blood vessels has severe effects, since the vasculature supplies nutrients to downstream organ systems. Experts in the field have conceded that flawed methodology, such as overreliance on the nonspecific marker α-SMA to identify SMCs or the habit of expanding and passaging SMCs at length before use in experiments, has become commonplace and often confounds results. In addition, bulk techniques often mask subtleties in cellular response. The question of SMC heterogeneity can only be resolved through single-cell analysis of SMCs.

Remarkably, single-cell analysis of functional contractility demonstrated that the expression level of contractile proteins such as α-SMA, CNN1, and SMMHC did not correlate with the force of cell traction or contraction exhibited by the same individual SMCs. Level of contractile force may be more dependent on other signaling molecules than the production of actin or myosin; therefore, although contractile state is often used to describe the phenotype of SMCs in vascular disease, it may be incorrectly associated with the pathogenic behavior observed in SMCs. To directly analyze behavioral differences among SMCs, a platform was established to integrate optoelectronic tweezers and a micropatterned substrate of ECM islands surrounded by PEG. OET was used to manipulate cells with single-cell resolution, and the specialized substrate was used for clonal culture of single cells. Compared to the random seeding of other single-cell techniques, OET dramatically enhanced the efficiency of single-cell positioning. OET was used to select and position SMCs, which were derived from the aorta of SMMHC-CreER^{T2}/LoxP-tdTomato transgenic mice and were thus labeled with red fluorescence. Single-cell clones were tracked, and two subpopulations of SMCs emerged: proliferative SMCs that were capable of undergoing osteogenic differentiation and a majority of SMCs that did not proliferate or differentiate. Thus, single-cell behavioral analysis of SMCs suggested that SMCs are naturally heterogeneous. Proliferation of a minority subpopulation of SMCs did not discount dedifferentiation; rather, it is possible that only a subset of SMCs is capable of undergoing dedifferentiation to become proliferative. This would suggest that SMC dedifferentiation and SMC heterogeneity coexist: the majority of SMCs are terminally differentiated, but a phenotypically plastic subpopulation of SMCs can dedifferentiate, proliferate, and differentiate into osteoblasts. The concept was further reinforced by single-cell analysis of protein expression through single-cell Western blotting. SMCs were dissociated from native ECM and directly analyzed without exposure to culture. Each SMC was probed for SMMHC, CNN1, and α-SMA, and in the 3D plot, the relationship between SMMHC and α-SMA was the most influential to clustering. SMCs from primary culture were also co-stained for SMMHC and α-SMA, and through clonal culture, information on the proliferative potential of each SMC could also be correlated. The clusters in immunostaining intensity closely matched the subpopulations of SMCs based on proliferative potential. Thus, differential behavior was correlated with differential protein expression. Furthermore, the clusters from single-cell Western blotting of SMMHC versus α-SMA exactly matched the clusters from immunostaining. In other words, the protein expression profiles of SMCs in primary culture accurately reflected the demographics of SMCs in normal vasculature. Consequently, the subpopulations of SMCs with different potential for proliferation and differentiation constitute

a heterogeneous media layer in the normal blood vessel wall. The majority of SMCs in the vessel wall are inactive and terminally differentiated, but a subpopulation of phenotypically plastic SMCs may respond to perturbation with proliferation, migration, and widespread mineralization during the development of vascular disease.

References

1 Mozaffarian, D. *et al.* Heart Disease and Stroke Statistics-2016 Update A Report From the American Heart Association. *Circulation* **133**, E38-E360 (2016).

2 Ross, R. The pathogenesis of atherosclerosis: a perspective for the 1990s. *Nature* **362**, 801-809, doi:10.1038/362801a0 (1993).

3 Owens, G. K. Regulation of Differentiation of Vascular Smooth-Muscle Cells. *Physiol Rev* **75**, 487-517 (1995).

4 Bennett, M. R., Sinha, S. & Owens, G. K. Vascular Smooth Muscle Cells in Atherosclerosis. *Circ Res* **118**, 692-702 (2016).

5 Chamley-Campbell, J., Campbell, G. R. & Ross, R. The smooth muscle cell in culture. *Physiol Rev* **59**, 1-61 (1979).

6 Bochaton-Piallat, M. L. Smooth muscle cell heterogeneity: implications for atherosclerosis and restenosis. *Eur J Clin Invest* **38**, 30-31 (2008).

7 Benditt, E. P. & Benditt, J. M. Evidence for a Monoclonal Origin of Human Atherosclerotic Plaques. *P Natl Acad Sci USA* **70**, 1753-1756 (1973).

8 Schwartz, S. M. & Murry, C. E. Proliferation and the monoclonal origins of atherosclerotic lesions. *Annu Rev Med* **49**, 437-+ (1998).

9 Chappell, J. *et al.* Extensive Proliferation of a Subset of Differentiated, yet Plastic, Medial Vascular Smooth Muscle Cells Contributes to Neointimal Formation in Mouse Injury and Atherosclerosis Models. *Circ Res* **119**, 1313-1323, doi:10.1161/CIRCRESAHA.116.309799 (2016).

10 Owens, G. K., Kumar, M. S. & Wamhoff, B. R. Molecular regulation of vascular smooth muscle cell differentiation in development and disease. *Physiol Rev* **84**, 767-801 (2004).

11 Regan, C. P., Adam, P. J., Madsen, C. S. & Owens, G. K. Molecular mechanisms of decreased smooth muscle differentiation marker expression after vascular injury. *Journal of Clinical Investigation* **106**, 1139-1147 (2000).

12 Neuhaus, J., Heinrich, M., Schwalenberg, T. & Stolzenburg, J. U. Cytokines Regulate the Expression of Connexins and Alpha-Smooth Muscle Cell Actin in Cultured Human Suburothelial Myofibroblasts. *Eur Urol Suppl* **8**, 274-274 (2009).

13 Ludin, A. *et al.* Monocytes-macrophages that express alpha-smooth muscle actin preserve primitive hematopoietic cells in the bone marrow. *Nat Immunol* **13**, 1072-1082 (2012).

14 Chiou, P. Y., Ohta, A. T. & Wu, M. C. Massively parallel manipulation of single cells and microparticles using optical images. *Nature* **436**, 370-372 (2005).

15 Pohl, H. A. *Dielectrophoresis : the behavior of neutral matter in nonuniform electric fields*. (Cambridge University Press, 1978).

16 Gascoyne, P. R. C., Becker, F. F. & Wang, X. B. Numerical-Analysis of the Influence of Experimental Conditions on the Accuracy of Dielectric Parameters Derived from Electrorotation Measurements. *Bioelectroch Bioener* **36**, 115-125 (1995).

17 Trainor, K., Morley, A. & Seshadri, R. Cloning of Lymphocytes at Limiting Dilution. *Clin Exp Pharmacol P* **10**, 466-467 (1983).

18 Underwood, P. A. & Bean, P. A. Hazards of the Limiting-Dilution Method of Cloning Hybridomas. *J Immunol Methods* **107**, 119-128 (1988).

19 Dvir-Ginzberg, M., Gamlieli-Bonshtein, I., Agbaria, R. & Cohen, S. Liver tissue engineering within alginate scaffolds: Effects of cell-seeding density on hepatocyte viability, morphology, and function. *Tissue Eng* **9**, 757-766 (2003).

20 Zhou, H. Z., Weir, M. D. & Xu, H. H. K. Effect of Cell Seeding Density on Proliferation and Osteodifferentiation of Umbilical Cord Stem Cells on Calcium Phosphate Cement-Fiber Scaffold. *Tissue Eng Pt A* **17**, 2603-2613 (2011).

21 Bonner, W. A., Sweet, R. G., Hulett, H. R. & Herzenberg, L. A. Fluorescence Activated Cell Sorting. *Rev Sci Instrum* **43**, 404-+ (1972).

22 Rettig, J. R. & Folch, A. Large-scale single-cell trapping and imaging using microwell arrays. *Anal Chem* **77**, 5628-5634 (2005).

23 Di Carlo, D., Wu, L. Y. & Lee, L. P. Dynamic single cell culture array. *Lab Chip* **6**, 1445-1449 (2006).

24 Ohta, A. T. *et al.* Dynamic cell and microparticle control via optoelectronic tweezers. *J Microelectromech S* **16**, 491-499 (2007).

25 Jamshidi, A. *et al.* Dynamic manipulation and separation of individual semiconducting and metallic nanowires. *Nat Photonics* **2**, 85-89 (2008).

26 Valley, J. K. *et al.* Parallel single-cell light-induced electroporation and dielectrophoretic manipulation. *Lab Chip* **9**, 1714-1720 (2009).

27 Valley, J. K. *et al.* Preimplantation Mouse Embryo Selection Guided by Light-Induced Dielectrophoresis. *Plos One* **5** (2010).

28 Ohta, A. T. *et al.* Motile and non-motile sperm diagnostic manipulation using optoelectronic tweezers. *Lab Chip* **10**, 3213-3217 (2010).

29 Hsu, H. Y. *et al.* Thermo-sensitive Microgels as in-situ Sensor for Temperature Measurement in Optoelectronic Tweezers. *Proc Ieee Micr Elect*, 1123-1126 (2010).

30 Damink, L. H. H. O. *et al.* Cross-linking of dermal sheep collagen using a water-soluble carbodiimide. *Biomaterials* **17**, 765-773 (1996).

31 Tengvall, P., Jansson, E., Askendal, A., Thomsen, P. & Gretzer, C. Preparation of multilayer plasma protein films on silicon by EDC/NHS coupling chemistry. *Colloid Surface B* **28**, 261-272 (2003).

32 Desai, N. P. & Hubbell, J. A. Solution Technique to Incorporate Polyethylene Oxide and Other Water-Soluble Polymers into Surfaces of Polymeric Biomaterials. *Biomaterials* **12**, 144-153 (1991).

33 Gombotz, W. R., Guanghui, W., Horbett, T. A. & Hoffman, A. S. Protein Adsorption to Poly(Ethylene Oxide) Surfaces. *J Biomed Mater Res* **25**, 1547-1562 (1991).

34 Lau, A. N. K. *et al.* Antifouling coatings for optoelectronic tweezers. *Lab Chip* **9**, 2952-2957 (2009).

35 Moon, S., Ceyhan, E., Gurkan, U. A. & Demirci, U. Statistical Modeling of Single Target Cell Encapsulation. *Plos One* **6** (2011).

36 Collins, D. J., Neild, A., deMello, A., Liu, A. Q. & Ai, Y. The Poisson distribution and beyond: methods for microfluidic droplet production and single cell encapsulation. *Lab Chip* **15**, 3439-3459 (2015).

37 Campbell, G. R. & Chamleycampbell, J. H. The Vascular Smooth-Muscle Cell in Culture. *Thromb Haemostasis* **46**, 77-77 (1981).

38 Campbell, J. H. & Campbell, G. R. Endothelial-Cell Influences on Vascular Smooth-Muscle Phenotype. *Annu Rev Physiol* **48**, 295-306 (1986).

39 Campbell, G. R., Campbell, J. H., Manderson, J. A., Horrigan, S. & Rennick, R. E. Arterial Smooth-Muscle - a Multifunctional Mesenchymal Cell. *Arch Pathol Lab Med* **112**, 977-986 (1988).

40 Kocher, O. *et al.* Phenotypic features of smooth muscle cells during the evolution of experimental carotid artery intimal thickening. Biochemical and morphologic studies. *Lab Invest* **65**, 459-470 (1991).

41 Kocher, O. & Gabbiani, G. Cytoskeletal features of normal and atheromatous human arterial smooth muscle cells. *Hum Pathol* **17**, 875-880 (1986).

42 Galis, Z. S., Sukhova, G. K., Lark, M. W. & Libby, P. Increased expression of matrix metalloproteinases and matrix degrading activity in vulnerable regions of human atherosclerotic plaques. *J Clin Invest* **94**, 2493-2503, doi:10.1172/JCI117619 (1994).

43 Wissler, R. W. The arterial medial cell, smooth muscle, or multifunctional mesenchyme? *Circulation* **36**, 1-4 (1967).

44 Gabbiani, G. *et al.* Vascular smooth muscle cells differ from other smooth muscle cells: predominance of vimentin filaments and a specific alpha-type actin. *Proc Natl Acad Sci U S A* **78**, 298-302 (1981).

45 Duband, J. L., Gimona, M., Scatena, M., Sartore, S. & Small, J. V. Calponin and SM 22 as differentiation markers of smooth muscle: spatiotemporal distribution during avian embryonic development. *Differentiation* **55**, 1-11 (1993).

46 Miano, J. M. & Olson, E. N. Expression of the smooth muscle cell calponin gene marks the early cardiac and smooth muscle cell lineages during mouse embryogenesis. *J Biol Chem* **271**, 7095-7103 (1996).

47 Werling, R. W., Hwang, H., Yaziji, H. & Gown, A. M. Immunohistochemical distinction of invasive from noninvasive breast lesions - A comparative study of p63 versus calponin and smooth muscle myosin heavy chain. *Am J Surg Pathol* **27**, 82-90 (2003).

48 Miano, J. M., Cserjesi, P., Ligon, K. L., Periasamy, M. & Olson, E. N. Smooth-Muscle Myosin Heavy-Chain Exclusively Marks the Smooth-Muscle Lineage during Mouse Embryogenesis. *Circ Res* **75**, 803-812 (1994).

49 Nemenoff, R. A. *et al.* SDF-1 alpha Induction in Mature Smooth Muscle Cells by Inactivation of PTEN Is a Critical Mediator of Exacerbated Injury-Induced Neointima Formation. *Arterioscl Throm Vas* **31**, 1300-U1138 (2011).

50 Shankman, L. S. *et al.* KLF4-dependent phenotypic modulation of smooth muscle cells has a key role in atherosclerotic plaque pathogenesis. *Nat Med* **21**, 628-637 (2015).

51 Feil, S. *et al.* Transdifferentiation of Vascular Smooth Muscle Cells to Macrophage-Like Cells During Atherogenesis. *Circ Res* **115**, 662-U159 (2014).

52 Mccaffrey, T. A., Nicholson, A. C., Szabo, P. E., Weksler, M. E. & Weksler, B. B. Aging and Arteriosclerosis - the Increased Proliferation of Arterial Smooth-Muscle Cells Isolated from Old Rats Is Associated with Increased Platelet-Derived Growth-Factor Like Activity. *J Exp Med* **167**, 163-174 (1988).

53 Stemerman, M. B. *et al.* Vascular smooth muscle cell growth kinetics in vivo in aged rats. *Proc Natl Acad Sci U S A* **79**, 3863-3866 (1982).

54 Hariri, R. J., Alonso, D. R., Hajjar, D. P., Coletti, D. & Weksler, M. E. Aging and arteriosclerosis. I. Development of myointimal hyperplasia after endothelial injury. *J Exp Med* **164**, 1171-1178 (1986).

55 BochatonPiallat, M. L., Ropraz, P., Gabbiani, F. & Gabbiani, G. Phenotypic heterogeneity of rat arterial smooth muscle cell clones - Implications for the development of experimental intimal thickening. *Arterioscl Throm Vas* **16**, 815-820 (1996).

56 Hao, H. *et al.* Heterogeneity of smooth muscle cell populations cultured from pig coronary artery. *Arterioscler Thromb Vasc Biol* **22**, 1093-1099 (2002).

57 Benzakour, O. *et al.* Evidence for cultured human vascular smooth muscle cell heterogeneity: isolation of clonal cells and study of their growth characteristics. *Thromb Haemost* **75**, 854-858 (1996).

58 Li, S. *et al.* Innate diversity of adult human arterial smooth muscle cells: cloning of distinct subtypes from the internal thoracic artery. *Circ Res* **89**, 517-525 (2001).

59 Frid, M. G., Moiseeva, E. P. & Stenmark, K. R. Multiple phenotypically distinct smooth muscle cell populations exist in the adult and developing bovine pulmonary arterial media in vivo. *Circ Res* **75**, 669-681 (1994).

60 Li, Z., Cheng, H., Lederer, W. J., Froehlich, J. & Lakatta, E. G. Enhanced proliferation and migration and altered cytoskeletal proteins in early passage smooth muscle cells from young and old rat aortic explants. *Exp Mol Pathol* **64**, 1-11, doi:10.1006/exmp.1997.2204 (1997).

61 Wagers, A. J. & Weissman, I. L. Plasticity of adult stem cells. *Cell* **116**, 639-648 (2004).

62 Nicosia, R. F. & Villaschi, S. Rat Aortic Smooth-Muscle Cells Become Pericytes during Angiogenesis in-Vitro. *Lab Invest* **73**, 658-666 (1995).

63 Steitz, S. A. *et al.* Smooth muscle cell phenotypic transition associated with calcification: upregulation of Cbfa1 and downregulation of smooth muscle lineage markers. *Circ Res* **89**, 1147-1154 (2001).

64 Orlandi, A., Ropraz, P. & Gabbiani, G. Proliferative Activity and Alpha-Smooth Muscle Actin Expression in Cultured Rat Aortic Smooth-Muscle Cells Are Differently Modulated by Transforming Growth-Factor-Beta-1 and Heparin. *Exp Cell Res* **214**, 528-536 (1994).

65 Seidel, C. L., Helgason, T., Allen, J. C. & Wilson, C. Migratory abilities of different vascular cells from the tunica media of canine vessels. *Am J Physiol-Cell Ph* **272**, C847-C852 (1997).

66 Bochaton-Piallat, M. L. *et al.* Cultured arterial smooth muscle cells maintain distinct phenotypes when implanted into carotid artery. *Arterioscl Throm Vas* **21**, 949-954 (2001).

67 Rong, J. X., Shapiro, M., Trogan, E. & Fisher, E. A. Transdifferentiation of mouse aortic smooth muscle cells to a macrophage-like state after cholesterol loading. *P Natl Acad Sci USA* **100**, 13531-13536 (2003).

68 Tseng, P., Pushkarsky, I. & Di Carlo, D. Metallization and Biopatterning on Ultra-Flexible Substrates via Dextran Sacrificial Layers. *Plos One* **9** (2014).

69 Yanagisawa, M., Kurihara, H., Kimura, S., Goto, K. & Masaki, T. Endothelin - a Novel Potent Vasoconstrictor Peptide Produced by Vascular Endothelial-Cells. *Faseb J* **2**, A393-A393 (1988).

70 Alves, R. D. A. M., Eijken, M., van de Peppel, J. & van Leeuwen, J. P. T. M. Calcifying vascular smooth muscle cells and osteoblasts: independent cell types exhibiting extracellular matrix and biomineralization-related mimicries. *Bmc Genomics* **15** (2014).

71 Steitz, S. A. *et al.* Smooth muscle cell phenotypic transition associated with calcification - Upregulation of Cbfa1 and downregulation of smooth muscle lineage markers. *Circ Res* **89**, 1147-1154 (2001).

72 Tanaka, T. *et al.* Runx2 represses myocardin-mediated differentiation and facilitates osteogenic conversion of vascular smooth muscle cells. *Mol Cell Biol* **28**, 1147-1160 (2008).

73 Trion, A., Schutte-Bart, C., Bax, W. H., Jukema, J. W. & van der Laarse, A. Modulation of calcification of vascular smooth muscle cells in culture by calcium antagonists, statins, and their combination. *Mol Cell Biochem* **308**, 25-33 (2008).

74 Llorente-Cortes, V., Martinez-Gonzalez, J. & Badimon, L. LDL receptor-related protein mediates uptake of aggregated LDL in human vascular smooth muscle cells. *Arterioscl Throm Vas* **20**, 1572-1579 (2000).

75 Campbell, J. H., Reardon, M. F., Campbell, G. R. & Nestel, P. J. Metabolism of Atherogenic Lipoproteins by Smooth-Muscle Cells of Different Phenotype in Culture. *Arteriosclerosis* **5**, 318-328 (1985).

76 Birsoy, K., Chen, Z. & Friedman, J. Transcriptional regulation of adipogenesis by KLF4. *Cell Metab* **7**, 339-347, doi:10.1016/j.cmet.2008.02.001 (2008).

77 Cui, Q., Wang, G. J. & Balian, G. Steroid-induced adipogenesis in a pluripotential cell line from bone marrow. *J Bone Joint Surg Am* **79a**, 1054-1063 (1997).

78 Leboy, P. S., Beresford, J. N., Devlin, C. & Owen, M. E. Dexamethasone induction of osteoblast mRNAs in rat marrow stromal cell cultures. *J Cell Physiol* **146**, 370-378, doi:10.1002/jcp.1041460306 (1991).

79 Hungerford, J. E., Owens, G. K., Argraves, W. S. & Little, C. D. Development of the aortic vessel wall as defined by vascular smooth muscle and extracellular matrix markers. *Dev Biol* **178**, 375-392 (1996).

80 Sartore, S. *et al.* Contribution of adventitial fibroblasts to neointima formation and vascular remodeling - From innocent bystander to active participant. *Circ Res* **89**, 1111-1121 (2001).

81 Frid, M. G. *et al.* Myosin heavy-chain isoform composition and distribution in developing and adult human aortic smooth muscle. *J Vasc Res* **30**, 279-292 (1993).

82 Sartore, S. *et al.* Myosin Isoform Expression in Smooth-Muscle Cells during Physiological and Pathological Vascular Remodeling. *Journal of Vascular Research* **31**, 61-81 (1994).

83 Hughes, A. J. *et al.* Single-cell western blotting. *Nat Methods* **11**, 749-U794 (2014).